Project No. 01-59

# PROPOSED ENHANCEMENTS TO PAVEMENT ME DESIGN: IMPROVED CONSIDERATION OF THE INFLUENCE OF SUBGRADE SOILS SUSCEPTIBLE TO SHRINK/SWELL AND/OR FROST HEAVE ON PAVEMENT PERFORMANCE

## APPENDIX 4

DETERMINISTIC SHRINK-SWELL MODEL

MAY 2023

**TABLE OF CONTENTS**

## LISTO OF FIGURES

## LIST OF TABLES

# 4. SHRINK SWELL DETERMINISTIC MODEL

This document introduces the proposed framework for deterministically estimating the 1D shrink-swell volume change of soil exposed to time-varying climatic effects.

## 4.1. Summary

This chapter presents an improved framework for estimating the volume change of shrink-swell soils due to time-varying climatic effects using the Lytton et al. (2005) approach with the suction envelope models created by Vann and Houston (2021). The proposed framework for estimating soil volume change of shrink-swell soils as a function of time is presented with an example calculation with data from an AASHTO Long-Term Pavement Performance (LTPP) Seasonal Monitoring Program (SMP) section TX 48-1068 (FHWA, 1995), which is located approximately 80 miles northeast of Dallas, Texas. The framework presented is applicable to uncovered sites where the groundwater table effects are negligible, but it has been calibrated to account for covered areas and for the spatial variation between the pavement center and edges.

## 4.2. Objectives

The following objectives pertaining to the development of the deterministic shrink swell volume change model were accomplished:

- The following objectives were accomplished as part of this study:
- Review and choose the deterministic SSVC framework which is to be incorporated into the stochastic analysis.
- Development of a framework for stochastically estimating the volume change on shrink-swell soils using the previously developed models for random soil property generation and monthly TMI forecasting.
- Exploration of the stability and sensitivity of the proposed shrink-swell forecast model.
- A comparison of the proposed models to the existing engineering practice including the differences in the uncertainty and sensitivity of the estimates.
- Exploration of the potential implementation of the proposed stochastic shrink-swell soil volume change model to foundation and pavement performance analysis/design.

## 4.3. Deterministic Shrink-Swell Volume Change (SSVC)

The ability to estimate soil volume change as a function of time is a valuable tool in the design of shallow foundations of pavement structures. Specifically pertaining to pavement design, estimating soil volume change as a function of time allows for the prediction of the potential cumulative International Roughness Index (IRI). The time-varying volume change can also be a valuable tool in the forensic analysis of existing foundation movement of a lightly loaded structure on shallow footings.

The author and members of the ASU research team (Zapata and Mosawi) published a paper in 2021 in the Soil and Rocks International Journal of Geotechnical and Geoenviromental Engineering titled “An Improved Framework for Volume Change of Shrink/Swell Soils Subjected to Time-Varying Climatic Effects”. The paper presents an improved framework for estimating the volume change of shrink-swell soils due to time-varying climatic effects using the Lytton et al. (2005) approach with the suction envelope models created by Vann and Houston (2021). The proposed framework for estimating soil volume change of shrink-swell soils as a function of time is presented with an example calculation with data from an AASHTO Long-Term Pavement Performance (LTPP) Seasonal Monitoring Program (SMP) section TX 48-1068 (FHWA, 1995), which is located approximately 80 miles northeast of Dallas, Texas. The framework presented is applicable to uncovered sites where the groundwater table effects are negligible, but it has been calibrated to account for covered areas and for the spatial variation between the pavement center and edges.

### *4.3.1. Suction-Volume Change Relationships*

Direct laboratory measurements of the volume change potential of a soil help improve the estimation of potential volume change in the field. The 1-D oedometer "Response to Wetting Test" as described in ASTM D4546 is the common type of laboratory test for volume change determination. One key difference from the laboratory oedometer test compared to the field conditions the soil will experience is the final degree of saturation. The response to wetting test inundates the sample, driving to almost full saturation. However, it is the probability that the soil will reach this moisture level over the period of the structure/pavements design life is very low (Houston and Houston 2017).

A common method for volume change estimation is the Potential Vertical Rise published by the Texas Department of Transportation (TxDOT-12-E, 1978), which includes both empirical-based relationships and result from an oedometer test. In 2005, the Texas DOT updated the approach to determining the volume change of expansive soils using the work by Lytton et al. (2005), which encompassed a suction-based approach. The study concluded that the previous empirical-based approach significantly overestimated the soil heave and did not account for the shrinkage of the soil during dry climatic periods.

A thorough literature review of volume change estimates of unsaturated soil (odometer-based, or suction-based) was performed by Vann (2019). The authors of this paper have carefully reviewed this relative literature summary as part of the research leading up to this paper.

The evaluation of moisture-driven volume change of unsaturated clay soil requires consideration of the net normal ($p$) and the matric suction ($s$) stress states. For clays under relatively light confinement, increases in $s$ during drying will typically cause clays to decrease in volume (compress or shrink) and reductions in $s$ during wetting will cause increases in volume (expansion or swell). Clay soils at high net normal stress states can also reduce in volume (collapse) during wetting (Houston and Zhang, 2021; Nooray, 2017). The volumetric response is commonly expressed in terms of changes in void ratio ($e$), and the general relationship between $e$, $p$ and $s$ for clay soils is represented using three-dimensional (3D) state surfaces (Alonso et al., 1994, 1999; Delage & Graham, 1996; Fredlund & Morgernstern, 1976; Gens & Alonso, 1993; Gens et al., 2016; Wheeler & Sivakumar, 1995; Vu & Fredlund, 2004; Wray et al., 2005; Zhang & Lytton, 2009a, 2009b). For many foundation and pavement applications in engineering practice, vertical deformations govern the design which allow for the *e-p-s* relationship to be analyzed using one-dimensional (1D) at-rest ($K_0$) conditions - or at least the 1-D analyses provide adequate information for decision making (Adem & Vanapalli, 2013; Fredlund et al., 1980; Houston & Houston, 2018; Lytton, 1997; Nelson & Miller, 1992; Nelson et al., 2015; Overton et al., 2006).

The study presents a comparison of the matric suction-volume change indices (for 1-D monotonic loading by wetting or drying) of intact clays (natural soil stress states) using relatively undisturbed specimens tested by Olaiz (2017), to those of reconstituted/compacted specimens measured by Singhal (2010) and Mosawi (2022) using OPPDs, including the Fredlund SWCC (SWC-150) developed by GCTS in Tempe, AZ. Singhal (2010) created a unique database from laboratory measurement of the mechanical response of clay soils under imposed conditions of both stress state variables using the OPPD, with attention on evaluation of a substantial portion of the void ratio state surface for clay soils. Olaiz (2017) and Mosawi (2022) continued the exploration of testing relatively intact and reconstituted soil specimens in the OPPD, respectively. The materials tested by Olaiz and Mosawi were obtained from locations associated with expansive soil areas in San Antonio, TX, and Denver, CO (same study sites previously analyzed in this document). The compilation of data from these extensive laboratory efforts was used to provide qualitative and quantitative comparisons of the mechanical response of reconstituted to relatively intact specimens.

The comparison of the matric suction-volume change indices of the intact samples from Olaiz (2017) resulted in significantly lower magnitude volume change than those of the remolded samples tested by Singhal (2010) and Mosawi (2022) for similar range of *wPI* specimens and suction range. A brief statistical analysis using descriptive

statistics, box plots, and 1:1 comparison indicated that for the compiled dataset, *wPI* provides a useful indicator for volumetric response for remolded specimens under relatively light confining stress. The data also demonstrated the critical role of stress history in shrink/swell response of clays to changes in moisture state. The data from the two-stress state controlled OPPD results provides a substantial start for development of *e-p-s* relationships and correlations for expansive clay soils.

### 4.4. Framework Outline

The following outline summarizes the steps of the improved framework for estimating the volume change of shrink/swell soils due to time-varying (monthly) climatic effects:

1. Weather station identification and data extraction
2. 30-year and monthly Thornthwaite Moisture Index per Witczak et al. (2006)
3. Determination of equilibrium suction envelope parameters per Vann and Houston (2021): depth to equilibrium suction and magnitude of equilibrium suction
4. Back-calculation of variables for Mitchell's (1979) equation
5. Development of long-term wet and dry suction profiles
6. Initial estimation of monthly changes in suction at the surface per Perera (2003)
7. Fourier equation fit to the monthly suction change at the surface.
8. Generation of monthly suction profile
9. Suction profile adjustments for varying surface boundary conditions
10. Calculation of net normal stress profile
11. Estimation of suction compression index (assuming value is not directly measured)
12. Calculation of strain monthly
13. Calculation of volume change monthly

The above deterministic framework is used in the stochastic analysis presented herein. Figure 4-1 presents a flow chart for the deterministic SSVC procedure.

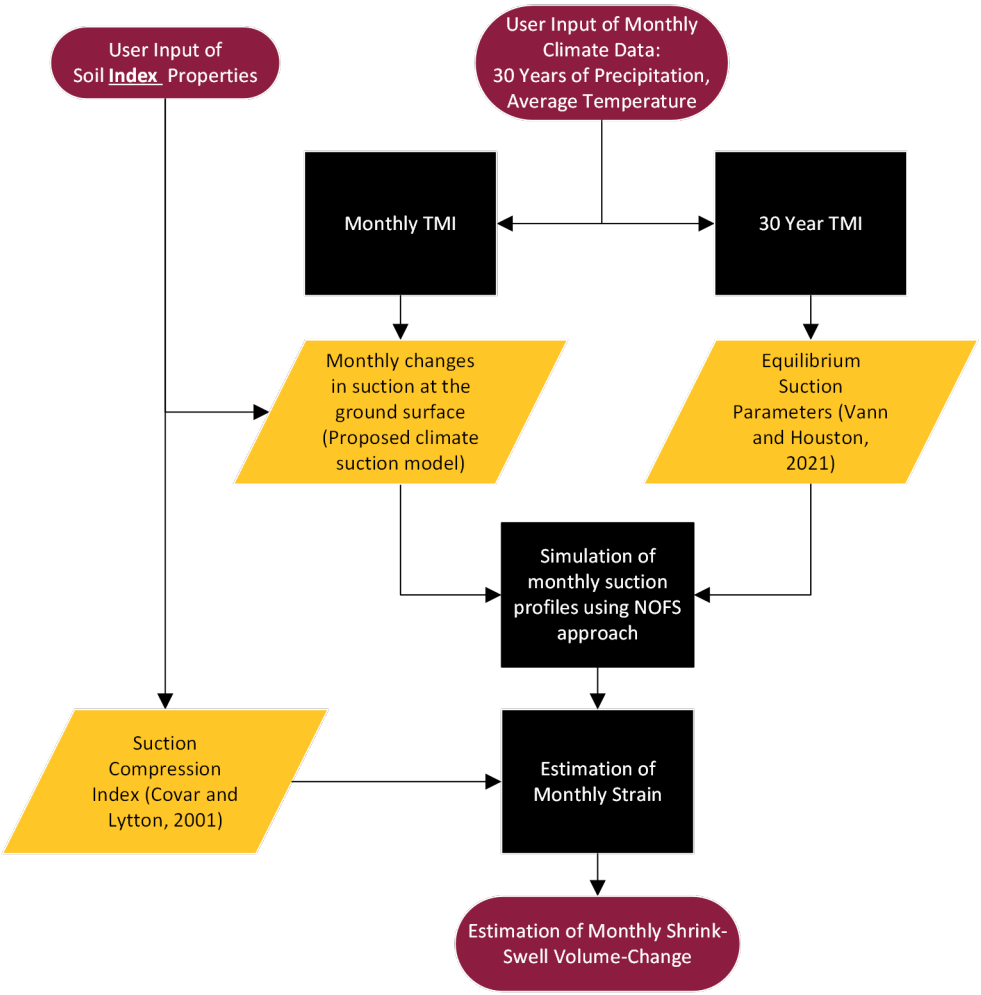


**Figure 4-1 Flow of the Deterministic SSVC Analysis Procedure**

*Step 1: Climate Data*

An SMP pavement section approximately 80 miles northwest of Dallas, Texas (TX 48-1068) is used to provide an example for the proposed framework. For the purposes of this example calculation, the climate data was gathered from the weather station nearest to the site and identified using the open-access Thornthwaite Moisture Index (TMI) GIS map developed by Olaiz et al. (2017), which uses the National Oceanic and Atmospheric Administration's (NOAA) 30-year climate normal database for the United States. Figure 4-2 below presents an excerpt for the GIS map, which has the Paris, TX weather station selected.

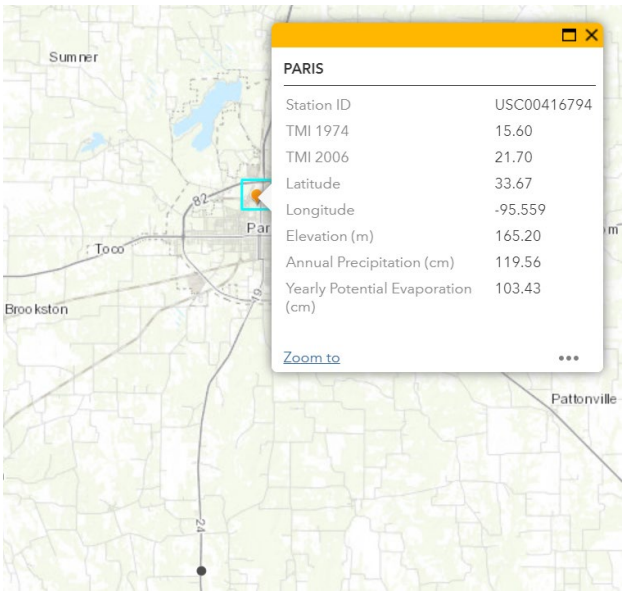


**Figure 4-2: Paris, TX weather station (NOAA ID USC00416794) data from online TMI GIS map (Olaiz et al., 2017)**

The "Station ID" shown in the pop-up window in **Figure** 4-**2** (USC00416794) is the only data needed for the purposes of this study. However, the remaining data shown may be helpful to get an understanding of the general climatic conditions at the site.

The NOAA climate data associated with each station in the country can be extracted from the online NOAA FTP site. It is recommended that the extracted weather data be filtered to contain the necessary variables for computation of the Thornthwaite Moisture Index (Witczak et al., 2006):

- Year
- Month
- Monthly Precipitation (cm)
- Monthly Average Temperature (Celsius)

Note that the Vann and Houston (2021) models used in the proposed analysis correlate the suction envelope parameters to a 30-year TMI value. As such, the climate data from the NOAA database for station USC00416794 was extracted for the date range of 9/1967 to 9/1997 (the last date of measured data from the SMP study for the TX 48-1068 section).

*Step 2: Monthly and 30-year Thornthwaite Moisture Index (Witczak et al., 2006)*

To determine yearly TMI for each month, first the potential evapotranspiration (*PET*) for each month must be calculated.

$$PET(cm) = f_1 f_2 1.6\left(\frac{10t}{I}\right)^a \tag{4-1}$$

where,

$f_1$ is the fraction of the number of days in month divided by the average number of days in month, 30; $f_2$ is the fraction

of the number of hours in a day divided by the base of 12 h in a day; $t$ is the mean monthly temperature in degrees Celsius; $I$ is the annual heat index; and $a$ is a coefficient.

$$I = \sum_{i=1}^{12} \left( \frac{t_i}{5} \right)^{1.514} \tag{4-2}$$

Where,

$t_i$ is the mean temperature for the $i^{th}$ month, and

$$a = 6.75 I^3 x 10^{-7} - 7.71 I^3 x 10^{-5} 1.792 I x 10^{-2} + 0.49239 \tag{4-3}$$

The TMI (Witczak et al., 2006) can now be determined by

$$TMI = 75 \left( \frac{P}{PET} - 1 \right) + 10 \tag{4-4}$$

where,

$P$ is the precipitation for the given month.

To visualize the climate data over time, the monthly average temperature, monthly rainfall, and the calculated TMI can be plotted (Figure 4-3). For the example calculation at the TX 48-1068 SMP section, the 30-year weather data must be analyzed (9/1967 to 9/1997). The duration which measured elevation change data was collected by SMP (3/1987 to 9/1997) is also analyzed for the example calculation so that measured vs. predicted values can be compared.

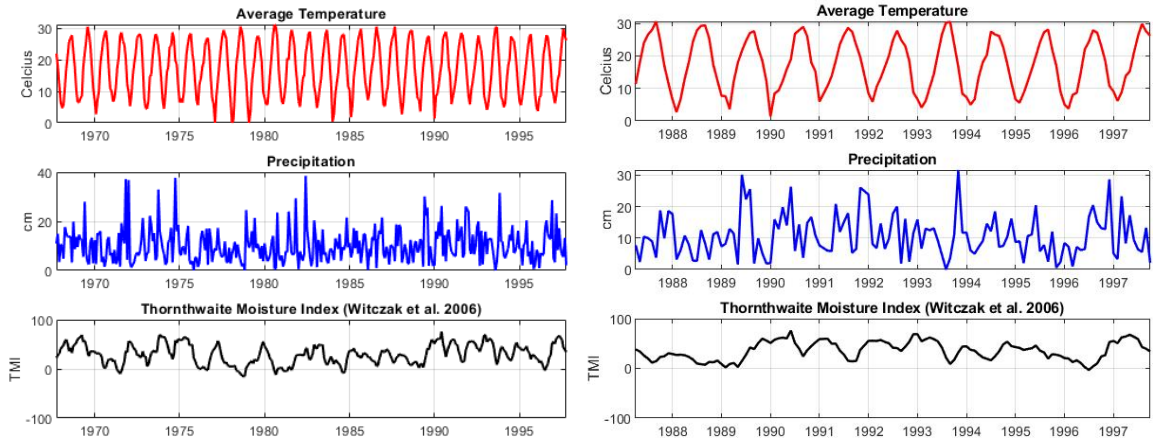


**Figure 4-3: Monthly average temperature and rainfall data for NOAA weather station USC00416794 with the calculated yearly TMI (Witczak et al, 2006) between a.) 9/1967 and 9/1997 and b.) 3/1987 and 9/1997.**

The 30-year TMI value (Witczak at al., 2006) calculated from the NOAA data set for the USC00416794 station is +29.6. This value does differ slightly from the +21.7 value previously shown on the TMI GIS map (**Figure 2**) due to the difference in date ranges used in the Olaiz et al. (2017) study.

*Step 3: Suction Envelope Parameters (Vann and Houston, 2021)*

The suction envelope defines the maximum and minimum suction values at the surface and within the subsurface to a depth of stable suction. The suction envelopes are established using the following parameters: (1) equilibrium suction, $\psi_e$, (2) depth to equilibrium suction, $D_{\psi_e}$, (3) change in suction at the ground surface, $\Delta\psi$, and (4) climate parameter, r.

The depth at which the climate-driven fluctuations in soil suction begins to stabilize, or equilibrate is determined using the Vann and Houston (2021) model (Figure 4-4) relatively flat uncovered sites subjected to natural climate surface flux conditions:

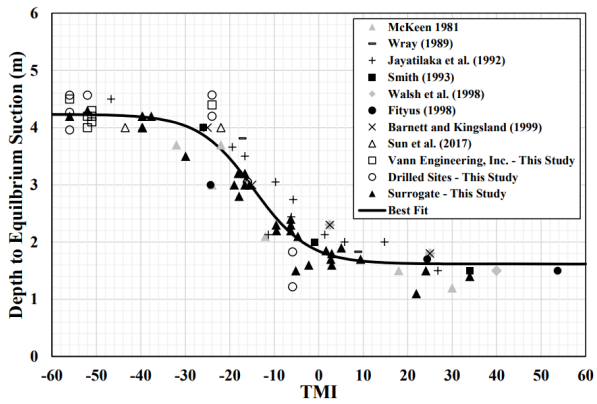


**Figure 4-4: Relationship between TMI and the depth to constant soil suction for uncovered and non-irrigated sites (Vann and Houston, 2021)**

The equation for the Depth to Equilibrium Suction ( $D_{\psi_e}$) versus TMI regression shown above is:

$$D_{\psi_e} = 1.617 + \frac{2.617}{1+e^{(2.36+0.1612TMI)}} \qquad (4\text{-}5)$$

With an $R^2 = 0.9045$ and standard error = 0.3147 m.

The stable, or equilibrium, suction value is determined using the Vann and Houston (2021) model (Figure 4-5). The soil suction unit of pF (log to the base 10 of soil suction in centimeters of water) was used in the Vann and Houston (2021) study due to its extensive use in the geotechnical practice, with regards to unsaturated soils. Note that log of suction in kPa units is approximately equal to suction in pF units, minus 1 (i.e., 4.0 pF = 3.0 log (suction (kPa)).

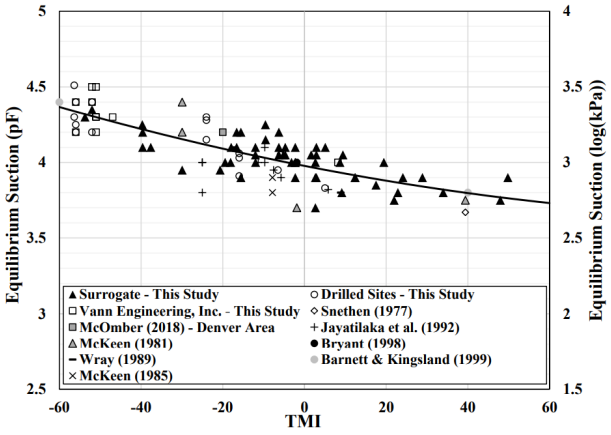


**Figure 4-5: Equilibrium Suction vs. TMI with Literature Values (Vann and Houston, 2021)**

The equation for the Equilibrium Suction ($\psi_e$) as a function of TMI is:

$$\psi_e\left(pF\right) = 0.0002TMI^2 - 0.0053TMI + 3.9771 \tag{4-6}$$

With an $R^2 = 0.6539$ and a standard error = 0.1959 pF.

The limits of the potential surface flux, or potential change in suction at the surface, is determined using the Vann and Houston (2021) model (Figure 4-6)

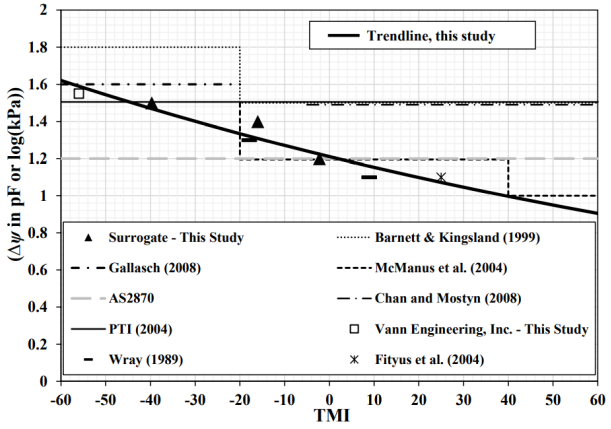


**Figure 4-6: Limits of the potential change in suction at the surface vs. TMI with literature values (Vann and Houston, 2021)**

The equation for the potential change in suction at the surface ($\Delta\psi$) as a function of TMI, as shown above is:

$$\Delta\psi\left(pF\right) = 1.2109e^{(-0.005TMI)} \tag{4-7}$$

With an $R^2 = 0.9184$ and a standard error = 0.1835 pF.

Aubeny and Long (2007) presented illustrative suction envelopes, developed from unsaturated flow analyses (Mitchell, 1980), to demonstrate that asymmetrical soil suction envelopes are expected, depending on the climate (TMI). Aubeny and Long introduced a climate parameter, r, that is the percentage of the total anticipated change in soil suction at the surface, ($\Delta\psi$), comprising the wet side of the suction envelope. The climatic parameter can be expressed in terms of the equilibrium suction and the minimum (wet) and maximum (dry) suction at the surface (z=0):

$$r = \frac{\left(\psi_e - \psi_{wet_{z=0}}\right)}{\left(\psi_{dry_{z=0}} - \psi_{wet_{z=0}}\right)} = \frac{\left(\psi_e - \psi_{wet_{z=0}}\right)}{\Delta\psi} \tag{4-8}$$

Houston and Vann created a relationship between the climatic parameter and TMI (Figure 4-7).

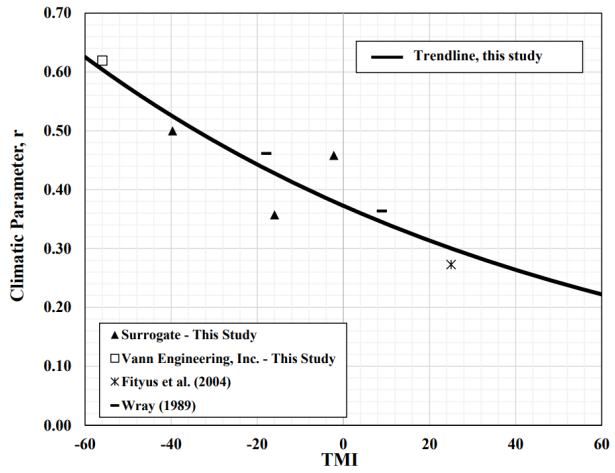


**Figure 4-7: Relationship between the Climate Parameter, r, and TMI (Vann and Houston, 2021)**

The equation for the climatic parameter ($r$) as a function of TMI as shown above is:

$$r = 0.3725e^{(-0.009TMI)} \tag{4-9}$$

With an $R^2 = 0.7998$ and a standard error = 0.1132.

Table 4-1 presents the suction envelope parameters for the SMP TX 48-1068 section which had 30-year TMI of 29.6.

**Table 4-1: Suction envelope parameters for the SMP TX 48-1068 per Vann and Houston (2021) with a TMI = 29.6**

| Suction Envelope Parameter | Value |
|---|---|
| Depth to Equilibrium Suction ( $D_{\psi_e}$ ) | 1.62 m |
| Equilibrium Suction ( $\psi_e$ ) | 3.84 pF |
| Change in suction at the surface ( $\Delta\psi$ ) | 1.044 pF |
| Climatic parameter (*r*) | 0.2854 |

*Step 4: Back Calculation of variables for Mitchell's equation (1980)*

The suction envelope can now be generated using the simplified unsaturated flow equation derived by Mitchell in 1980. The adjustment to the equation by Aubeny and Long (2007) for asymmetrical suction envelopes has also been incorporated into this study.

The Mitchell (1979) equation for change in suction with depth and time, simplified by Naiser (1997) to consider only the extreme suction cases (wet and dry), by taking the time variable to infinity, is used to obtain the shape of the envelopes.

$$\psi(z) = \psi_e + \Delta\psi e^{\left(-z\sqrt{\frac{n\pi}{\alpha}}\right)} \tag{4-10}$$

where,

$\psi$ is units of pF and z, *n* and $\alpha$ are in consistent units, $\psi$(z) is the suction value at any depth *z, n* is the frequency of suction cycles, and $\alpha$ is the diffusion coefficient.

The suction change with depth is a function of change in suction at the surface ($\Delta\psi\ in\ pF\ units$) and the equilibrium suction ($\psi_e$).

Once the key parameters of the profiles are established for any given TMI, all information required for the Mitchell (1980) flow computations (such as the ratio of the diffusion coefficient to the number of seasonal cycles per year) can be back-calculated (Vann, 2019). The n, α, π terms in the Mitchell (1981) equation, are back-calculated using the known equilibrium depth, $D_{\psi_e}$, change in suction at surface, $\Delta\psi$, and the 0.2 pF difference (Lytton, Aubeny, and Long, 2005; Vann 2019), wet to dry, at the depth of equilibrium.

$$\frac{n\pi}{\alpha} = \left( \frac{\ln\left(\frac{0.2\,pF}{\Delta\psi}\right)}{-D_{\psi_e}} \right)^2 \tag{4-11}$$

The suction profile can now be generated using equations 10 and 11 and the previously computed components of the surrogate suction, where suction is in pF units and depth is in meters.

*Step 5: Development of the wet and dry suction envelope*

The suction envelope defines the boundary conditions for the suction value at any depth within the soil profile. At the ground surface, the minimum (wet) and maximum (dry) suction values can be determined using the following expressions:

$$\psi_{wet_{z=0}} = \psi_e - r\Delta\psi \tag{4-12}$$

$$\psi_{dry_{z=0}} = \psi_{wet_{z=0}} + \Delta\psi \tag{4-13}$$

The minimum (wet) and maximum (dry) suctions for the TX 48-1068 section are 3.54 and 4.58, respectively.

The step size, or thickness of depth intervals (*dz*) must be determined. A sensitivity analysis should be performed to determine the number of steps ($n_z$) needed for the analysis; however, a value of 20 steps has been found to be sufficient for the volume change calculation performed in this study. The step size is computed by:

$$dz = \frac{D_{\psi_e}}{\left(n_z - 1\right)} \tag{4-14}$$

The step size for the SMP TX 48-1068 section is 8.526 cm using 20 steps with a depth of equilibrium suction of 1.62 m.

The wet and dry limit suction curves are iteratively calculated as the depth (*z*) is increased from 0 (ground surface) to the depth of equilibrium suction.

$$\psi\left(z_i\right)_{wet} = \psi_e - r\Delta\psi e^{\left(-z_i\sqrt{\frac{n\pi}{\alpha}}\right)} \tag{4-15}$$

$$\psi\left(z_i\right)_{dry} = \psi_e + \left(1-r\right)\Delta\psi e^{\left(-z_i\sqrt{\frac{n\pi}{\alpha}}\right)} \tag{4-16}$$

The suction for the SMP TX 48-1068 section is shown in Figure 4-8.

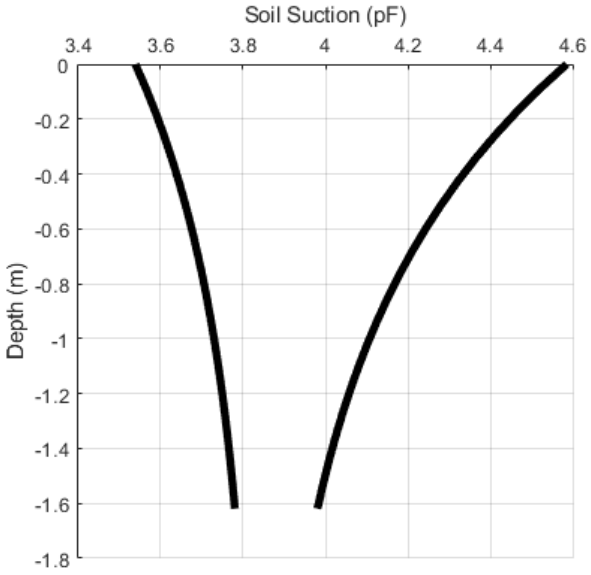


**Figure 4-8: Suction envelope for the SMP TX 48-1068 section using the Vann and Houston (2021) models**

*Step 6: Initial estimate of monthly changes in suction at the surface (Perera, 2003)*

It is important to note that the following steps for determining the suction at the surface over time are specific to a deterministic approach for estimating historic ground movements. Such approach can be used for a case study, forensic analysis, or calibration efforts based on measured data. The suction at the surface over time can also be modeled using a stochastic analysis with randomly generated monthly TMI values based on the historic averages and standard deviations. The second type of analysis can be used for designs of future structures; however, an example of such analysis is not presented in this paper.

In 2003, Perera studied the relationship between in-situ moisture content, suction, TMI, and index soil properties. He developed correlations for two models: the *TMI-*$P_{200}$ model, which is valid for granular base materials; and the *TMI-*$P_{200}$*/wPI* model, used to estimate the equilibrium suction of subbase and subgrade materials (Rosenbalm 2011). The two models are briefly explained in the following paragraphs.

The *TMI-P200/wPI* model is of interest to this study. This model was developed for fine-grained material, which makes it suitable for expansive soils. For such materials, in addition to $P_{200}$, the weighted plasticity index, *w*PI, property was added, where:

$$wPI = \left(\frac{P_{200}}{100}\right) PI \tag{4-17}$$

The wPI for the example in Paris, TX site is 18.4 based on the percent passing the #200 sieve of 74% and a PI of 20.

The following equation is used to calculate suction based TMI, $P_{200}$, and *w*PI (Perera 2003).

$$\Psi = \alpha\left[e^{\left[\frac{\beta}{TMI+\gamma}\right]} + \delta\right] \tag{4-18}$$

where, $\Psi$ is the matric suction of the soil; and $\alpha, \beta, \gamma, and\ \delta$ are regression constants.

Rosenbalm developed equations for each regression constant. These equations are used when *w*PI is less than 0.5 (Rosenbalm 2011):

$$\beta = 2.56075\left(P_{200}\right) + 393.4625 \tag{4-19}$$

$$\gamma = 0.09625\left(P_{200}\right) + 132.4875 \tag{4-20}$$

$$\delta = 0.025\left(P_{200}\right) + 14.75 \tag{4-21}$$

The following equations are used when *w*PI ≥ 0.5:

$$\beta = 0.006236\left(wPI\right)^3 - 0.7798334\left(wPI\right)^2 + 36.786486\left(wPI\right) + 501.9512 \tag{4-22}$$

$$\gamma = 0.00395\left(wPI\right)^3 - 0.04042\left(wPI\right)^2 + 1.454066\left(wPI\right) + 136.4775 \tag{4-23}$$

$$\delta = -0.01988\left(wPI\right)^2 + 1.27358\left(wPI\right) + 13.91244 \tag{4-24}$$

*Step 7: Adjustment to the estimation of monthly changes in suction at the surface (Vann and Houston (2021)*

It has been observed by the authors that the suction at the surface calculated using the Perera (2003) model typically will not reach the long-term minimum and maximum suction values observed by Vann and Houston (2021). This may not cause a significant issue if the analysis period is relatively short (e.g., less than ten years), however; for the purpose of pavement design, which typically incorporates a design life of 20+ years, it is recommended that the surface suction values determined from the Perera model be adjusted so that they will reach the limits observed by Vann and Houston (2021). This can be conducted by normalizing the maximum and minimum suction values from the Perera model to the previously computed potential change in suction at the surface ($\Delta\psi$).

$$\left(\psi_i\right)_{norm} = \left(\psi_{wet}\right)_{z=0} + \Delta\psi\left(\frac{\left(\psi_i\right)_{z=o} - \left(\psi_{Perra}\right)_{\min}}{\left(\psi_{Perra}\right)_{\max} - \left(\psi_{Perra}\right)_{\min}}\right) \tag{4-25}$$

After iterating the process for each month, the adjusted surface suction values can be plotted to help visualize

adjustment (Figure 4-9).

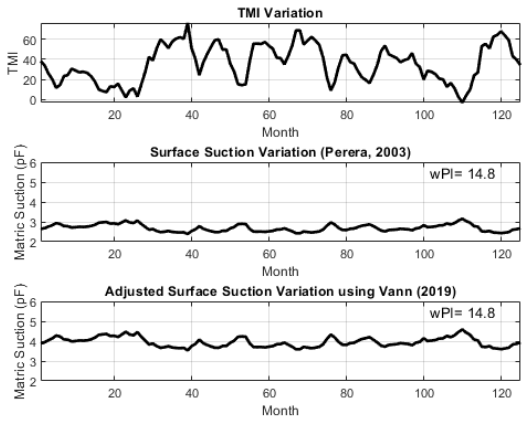


**Figure 4-9: Monthly TMI, Perera (2003) surface suction, and the Vann (2019) adjusted surface suction for the TX 48-1068 section for the date range 3/1987 to 9/1997**

*Step 8: Fourier equation fit to the monthly surface suction (Aubeny and Long, 2007)*

In order to model the suction changes as a function of time and depth, an equation must be developed to represent the variation of suction at the surface. Typically, a simple sinusoidal fit has been used to represent the surface suction variation with time. However, Aubeny and Long (2007), proposed that a Fourier transform can be used to improve the goodness of fit. As such, an 8th degree Fourier series is used in this analysis to fit an equation to the highly variable surface suction data.

In general, the Fourier series is a sum of sine and cosine functions that describes a periodic signal. It is represented in either the trigonometric form or the exponential form.

$$y = a_0 + \sum_{i=1}^{n} a_i \cos(iwx) + b_i \sin\left(iwx\right) \tag{4-26}$$

Where, $x$ represents time (for this analysis), $a_o$ models a constant (intercept) term in the data and is associated with the i = 0 cosine term, $w$ is the fundamental frequency of the signal, n is the number of terms (harmonics) in the series, and $1 \leq n \leq 8$, and $a_i$ and $b_i$ are the fitting parameters. Additional background information on the Fourier series can be found at: (https://www.mathworks.com/help/curvefit/fourier.html).

Figure 4-10 presents the 1st and 8th order Fourier fit to the Vann and Houston (2021) adjusted surface suction for the TX 48-1068. The 1st order fit closely represents the original approach to modeling the surface suction flux by Lytton et al. (2005) using Mitchell's (1979) equation. The adjusted $R^2$ for the 1st order Fourier fit to the suction data is 0.2903, while the 8th order Fourier fit increases the adjusted $R^2$ to 0.7056.

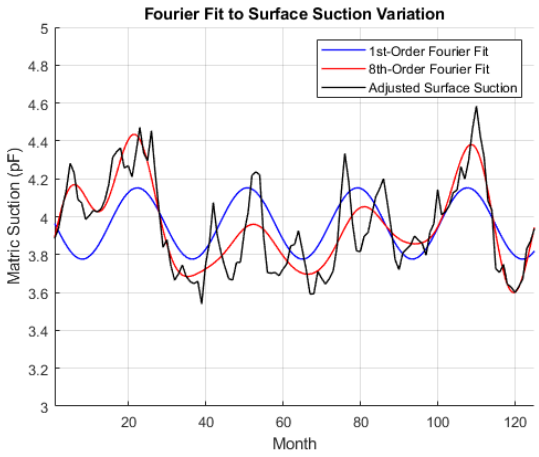


**Figure 4-10: 1st and 8th order Fourier fit to the surface suction data for the TX 48-1068 section for the date range 3/1987 to 9/1997**

One limitation of requiring an equation to represent the surface suction, is that generally the equation fit will not be able to encompass the maximum and minimum values of the individual monthly data. For purposes of the shrink/swell volume change analysis, the inclusion of the peaks of the surface suction can provide more accurate and conservative representation of extreme events. As such, the Fourier surface suction equation can be normalized between the maximum and minimum values of the surface suction; however, this additional step was not performed as part of the example analysis presented in this paper.

Note that the initial suction is a function of the TMI value for that month. The initial suction (time = 0), can be adjusted using a phase shift of the Fourier equation. Lytton et al. (2005), provided values of phase shifts for different initial conditions of the soil (wet, dry, and equilibrium). The example calculation in this report does not include the phase shift for the initial conditions.

*Step 9: Monthly Suction Profile (Aubeny and Long, 2007)*

The next step is to model the suction profile change with time using Aubeny and Long's (2007) adjusted 1979 Mitchell equation.

$$u(y,t) = U_e - (U_{dry} - U_{wet}) \sum_{k=1}^{\infty} \alpha_k \exp\left(-\sqrt{\lambda k}\right) \cos\left(\tau k - \sqrt{\lambda k}\right) \tag{4-27}$$

Where

$$y = depth, \quad \lambda = \pi y^2 n_\lambda / \alpha, \quad \tau = 2\pi t n_\lambda, \text{ and } \alpha_k = (2/k\pi)\sin(k\pi r) \quad k = 1,2,3...$$

For a given point in time, the suction profile can be estimated using the Aubeny and Long approach. Figure 4-11 presents the estimated suction at time = 1 month for the TX 48-1068 SMP site. Note that the long-term or extreme boundaries of the suction profile are known from the Vann (2019) correlations with the 30-year TMI value previously presented herein.

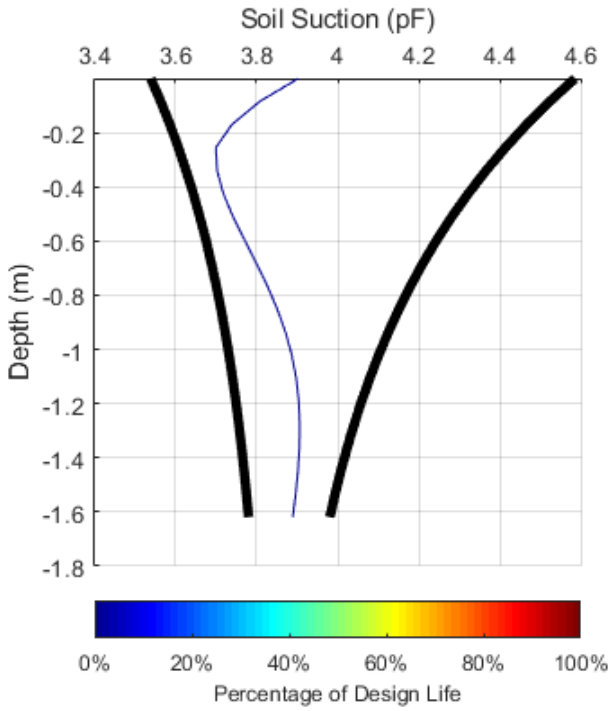


**Figure 4-11: The estimated initial suction profile (time = 1 month) for TX 48-1068 section**

The monthly change in suction at each depth can be determined by calculating the following months suction profile and taking the difference of the two values at each depth. It is this ongoing change in soil suction with time that drives the volume change of shrink/swell soils. Figure 4-12 shows the suction profiles for the initial state (t = 1 month) and the second month (t = 2 months) for the TX 48-1068 SMP site. Figure 4-13 shows the suction profiles for month 1 through month 12.

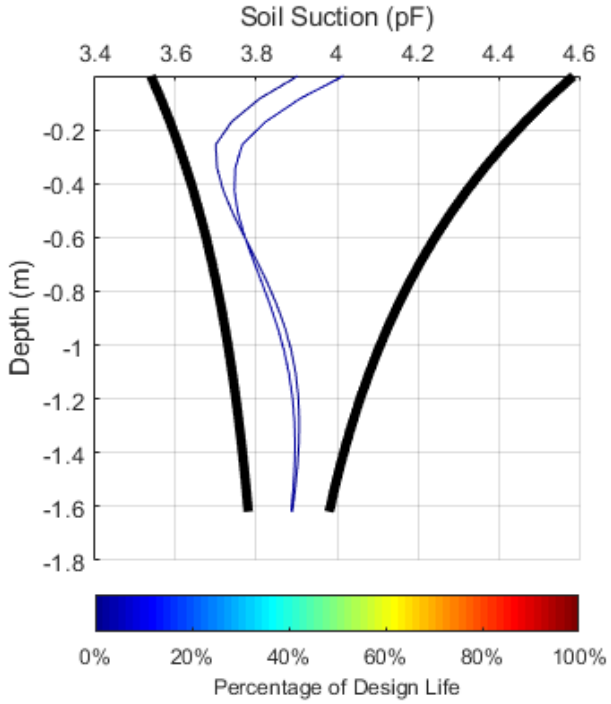


**Figure 4-12: The estimated initial suction profiles (time = 2 months) for TX 48-1068 section**

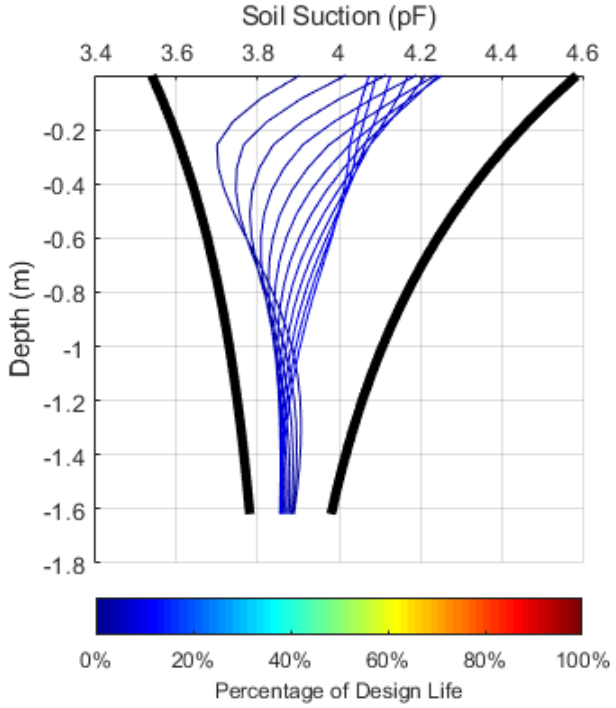


**Figure 4-13: The estimated initial suction profiles (time = 12 months) for TX 48-1068 SMP section**

**Figure 14** presents the monthly suction profiles over the date range 3/1987 to 9/1997 life for TX 48-1068 SMP section.

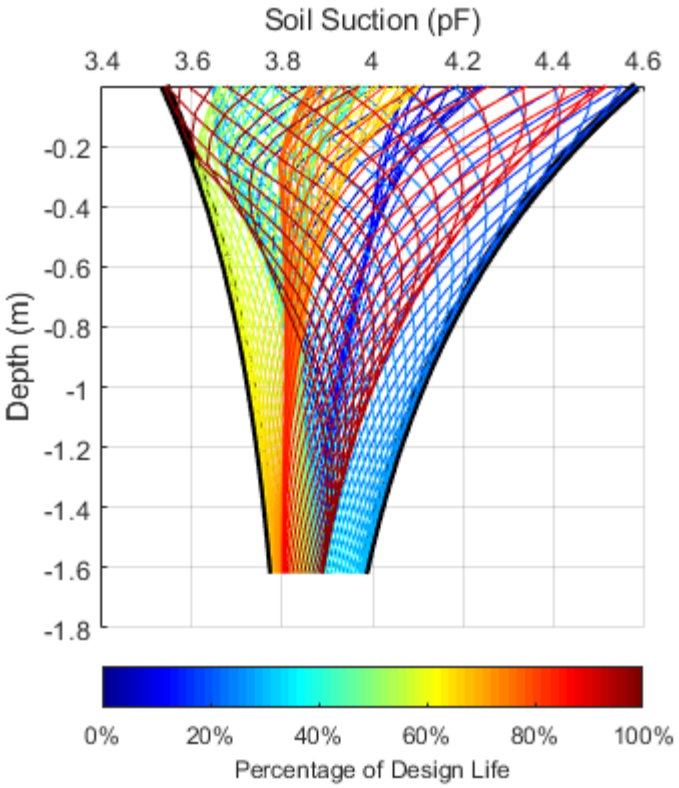


**Figure 4-14: Monthly suction profiles over the date range 3/1987 to 9/1997.**

From the figure, the significant swings of the suction profile from wet to dry, over the date range 3/1987 to 9/1997, can be observed. The monthly change in suction at each depth in the soil profile can be determined from this model.

To account for hysteresis effects associated with the wetting and drying of soil, it is important to record if the soil is wetting or drying at each depth and time during the iterative analysis. This information will be used during the strain calculation discussed later in this report.

*Step 10: Suction Profile Adjustments due Varying Boundary Conditions*

It is plausible that the subject site has a variable groundwater table, nearby vegetation, or is constructed using a moisture barrier. If any of these boundary conditions are present, the suction envelope and profile must be adjusted. (e.g. the suction profile will reach osmotic suction at the groundwater table depth). No variable boundary conditions were included in this example calculation.

*Step 11: Net Normal Stress Profile*

The net normal, or overburden stress, is a key component of shrink/swell volume change determination as it will help reduce potential soil swelling and can increase soil shrinkage. The overburden stress profile is determined using the conventional total stress approach.

$$\sigma_z = \sum(\gamma_{soil} z) \tag{4-28}$$

Note that the water content is subject to change over time as the soil suction changes, which will affect the magnitude of the net normal stress. However, for purposes of this example calculation, the effect of the changing water content on the net normal stress is negligible and is not included in the analysis.

If there are foundation loads or increases overburden stresses due to pavement layers above the subject soil profile, an increase of stress will be applied throughout the net normal stress profile.

*Step 12: Suction Compression Index (Covar and Lytton, 2001)*

The most widely accepted method for estimating volumetric strain is the one developed for the Texas DOT and the Federal Highway Administration, FHWA, by Lytton et al. in 2005, which is as follows:

$$\frac{\Delta V}{V} = -\gamma_h \log\left(\frac{h_f}{h_i}\right) - \gamma_\sigma \log\left(\frac{\sigma_f}{\sigma_i}\right) - \gamma_\pi \log\left(\frac{\pi_f}{\pi_i}\right) \tag{4-29}$$

Where, $\frac{\Delta V}{V}$ is the volumetric strain (volume change with respect to initial volume); $\gamma_h$ is the the matric suction compression index; $\gamma_\sigma$ is the mean principal stress compression index; $\gamma_\pi$ is the osmotic suction compression index; $h_i$ is the initial matric suction; $h_f$ is the final matric suction; $\sigma_i$is the initial mean principal stress; $\sigma_f$ is the final mean principal stress; $\pi_i$ is the initial osmotic suction; and $\pi_f$ is the final osmotic suction.

Although, total suction is the sum of matric suction and osmotic suction, Fredlund wrote "Matric suction in a soil mass change is a result of moisture infiltration and evaporation at the ground surface. Osmotic suction in the soil does not appear to be highly sensitive to modest changes in the water content of the soil. As a result, a change in the total suction is quite representative of a change in the matric suction." (Fredlund 2012). Also, Lytton wrote: "It is the change of matric suction that generates the heave and shrinkage, while osmotic suction rarely changes appreciably." (Lytton 2005) Thus, the change in matric suction is responsible to shrinkage and heave and osmotic suction does not affect enough to be concerned. (Lytton 2005, Fredlund 2012) Thus, the equation can be rewritten as:

$$\frac{\Delta V}{V} = -\gamma_h \log\left(\frac{h_f}{h_i}\right) - \gamma_\sigma \log\left(\frac{\sigma_f}{\sigma_i}\right) \tag{4-30}$$

Note that the net normal stress portion of the equation is added if the soil is wetting (swelling) and subtracted if the soil is drying (shrinking).

The Suction compression index, $\gamma_h$, is a parameter used to relate total suction to volume change to predict heave or shrinkage in expansive soils. This value can either be measured or estimated using soil index properties (Atterberg limits and gradation) as described in Covar and Lytton (2001).

First, the mineralogical zone is determined using Figure 4-15 with soils plasticity index (PI) and liquid limit (LL).

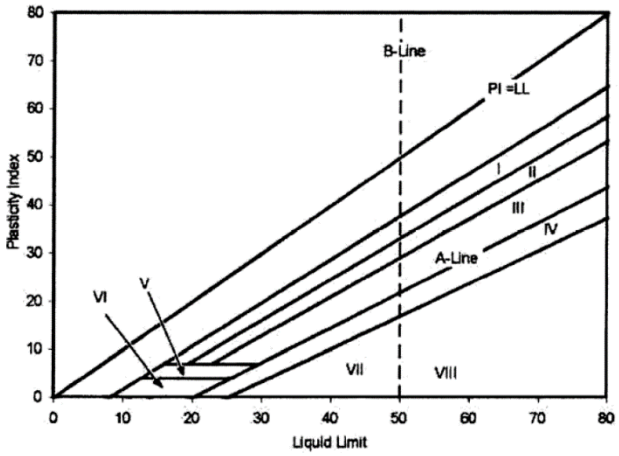


**Figure 4-15: Mineralogical zones for soil (Covar and Lytton, 2001)**

The zone for the TX 48-1068 SMP section site is Zone 2, using a LL = 60 and a PI = 40.

The percent fine clay (%fc) is then calculated using the percent passing #200 sieve ($P_{200}$) and the percent clay (%clay) obtained via hydrometer testing.

$$\%fc = \left( \frac{\%clay}{P_{200}} \right) \tag{4-31}$$

The %fc for the example site is 21.05%, using a %clay = 20% and $P_{200}$ = 95%.

The average suction compression index ($\gamma_0$) can now be determined using the charts developed by Covar and Lytton (2001), which are separated by mineralogical zones (Figure 4-16)

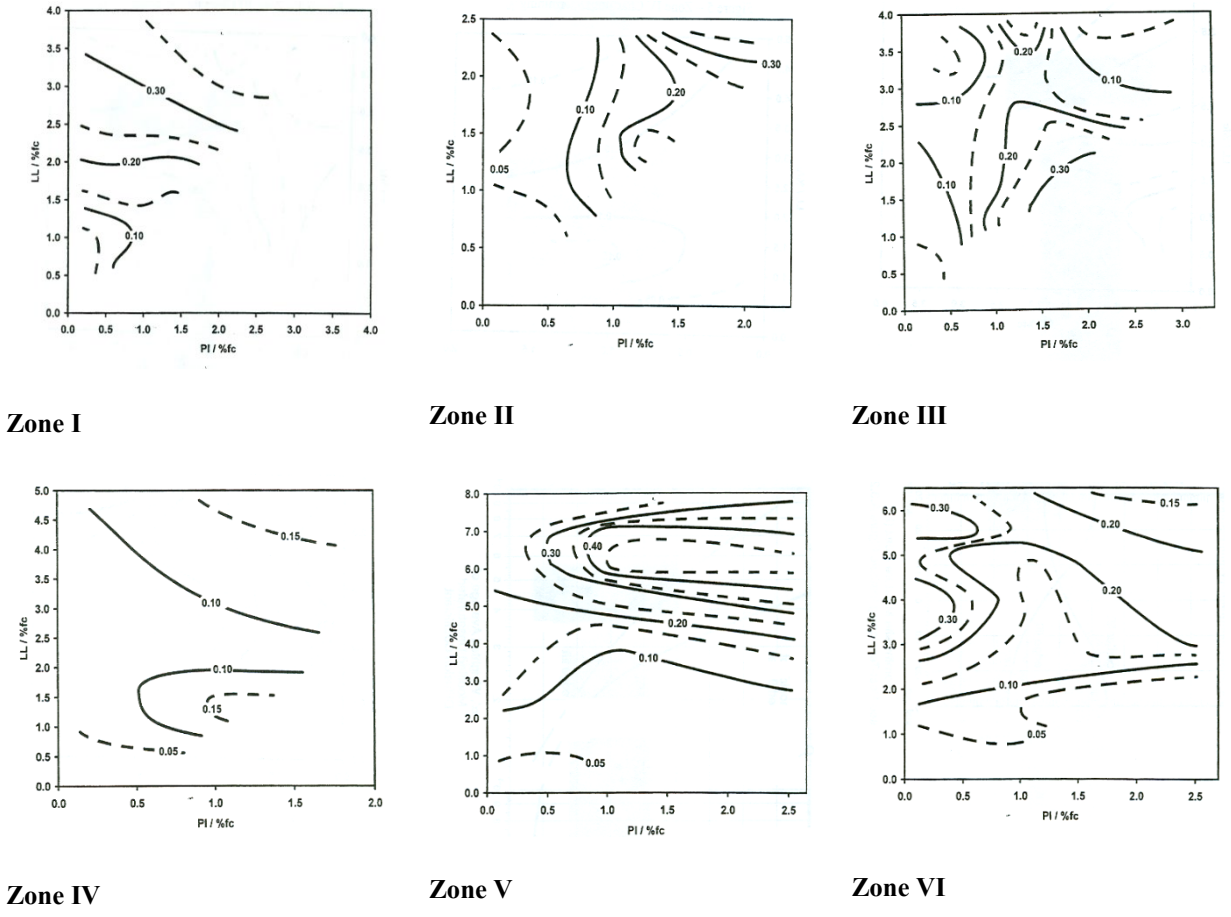


**Zone I** **Zone II** **Zone III**

**Zone IV** **Zone V** **Zone VI**

**Figure 4-16: Suction Compression Index based on Mineralogical Classification and Soil Index Properties (Covar and Lytton 2001)**

The average suction compression index for the TX 48-1098 SMP section is 0.051 using Zone 1, %fc = 43.78%, LL = 38, and PI = 20.

The adjusted suction compression index ($\gamma_h$) is now determined by:

$$\gamma_h = \gamma_0 \left(\%fc\right) \tag{4-32}$$

The adjusted suction compression index for TX 48-1098 SMP section site is 0.0223.

The hysteresis effects of the soil are now accounted for using the equations from the PTI (2006) Manual. The wetting and dying suction compression indices must be calculated for each depth and time of the analysis using the recorded wetting/drying information from Step 9.

$$\gamma_{swell} = \gamma_h e^{(\gamma_h)} \tag{4-33}$$

$$\gamma_{shrink} = \gamma_h e^{(-\gamma_h)} \tag{4-34}$$

*Step 13: Monthly Strain Calculation*

The mean principal stress compression index, $\gamma_\sigma$, can be calculated using its relation to the compression index, $C_c$, and void ratio, e, as follows (Lytton 2005):

$$\gamma_\sigma = \frac{C_c}{1+e_0} \tag{4-35}$$

Where, $C_c$ is the compression index; and $e_0$ is the void ratio. For purposes of this example calculation, the mean principal stress compression index was assumed to be 10% of the suction compression index as recommended by Lytton (2005).

The mean principal stress must be iteratively determined at each depth and time step, as it is a function of the net normal stress and the wetting/drying condition.

$$\sigma = \frac{1+2K_0}{3}\sigma_z \tag{4-36}$$

Where, $\sigma_z$ is the previously calculated vertical stress at a point below the surface in the soil mass; and $K_0$ is the 1-D at-rest lateral earth pressure coefficient.

$$K_0 = e\left(\frac{1-\sin(\phi')}{1+\sin(\phi')}\right)\left(\frac{1+d\sin(\phi')}{1-k\sin(\phi')}\right)^n \tag{4-37}$$

Values of coefficients *e, d, k, and n* for different soil conditions are given in Table 4-2.

**Table 4-2: Lateral Earth Pressure Parameter Coefficients**

| Conditions | $K_0$ | e | d | k | n |
|---|---|---|---|---|---|
| Cracked | 0 | 0 | 0 | 0 | 1 |
| Drying (Active) | 1/3 | 1 | 0 | 0 | 1 |
| Equilibrium (at rest) | 1/2 | 1 | 1 | 0 | 1 |
| Wetting (within movement active zone) | 2/3 | 1 | 1 | 0.5 | 1 |
| Wetting (below movement active zone) | 1 | 1 | 1 | 1 | 1 |
| Swelling near surface (passive earth pressure) | 3 | 1 | 1 | 1 | 2 |

The angle of internal friction, $\phi$', can be estimated from its empirical correlation with plasticity index, PI, based on triaxial compression tests.

$$\phi' = 0.0016PI^2 - 0.3021PI + 36.208 \tag{4-38}$$

The internal angle of friction for the TX 48-1068 SMP site is 30.8° using a PI = 20.

Using the data developed from the iterative steps discussed above, and the suction-overburden-strain relationships, the volume change over time can be estimated. Figure 4-17 presents the volume change estimation for the Paris, TX site.

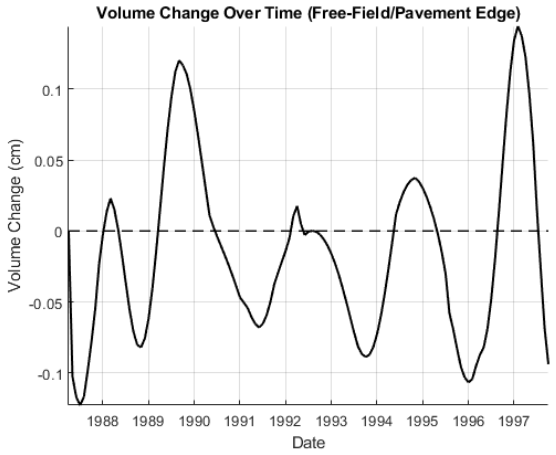


**Figure 4-17: Volume change over time for the TX 48-1068 site**

### *4.4.1. Estimated Volume Change Comparison to Measured Data*

The estimated volume change from the proposed framework for the TX 48-1068 site was compared to the measured data gathered from the LTTP SMP database. The estimated data was normalized to the value of the first measurement. Figure 4-18 presents the measured and estimated volume change for the TX 48-1068 SMP section.

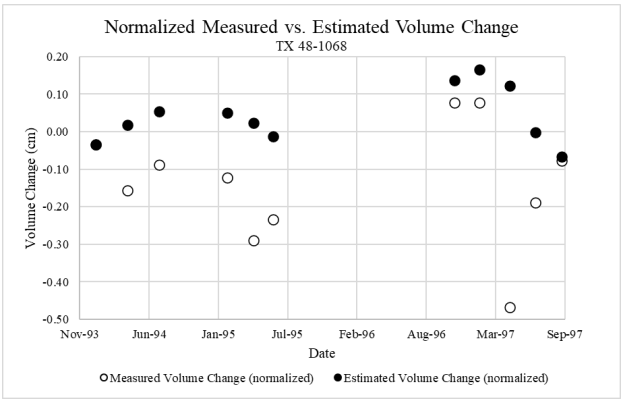


**Figure 4-18: Measured vs. Estimated Volume Change Normalized to the Initial Measurement for the TX 48-1068 SMP Section**

The authors are performing similar analysis with the remaining LTTP SMP sections so that calibration factors for the proposed framework can be obtained and further improve the estimation of the volume change.

### 4.5. 2D SSVC Estimates for Pavements

To account for covered areas, pavement or moisture barriers, a regression model was developed by Jayatilaka (1999) to estimate the vc movement using two programs developed by Gay (1994), MOPREC and FLODEF. The idea is to estimate the relationship between 1-D and 2-D vertical movement. Such analysis can be used to adjust suction profiles to consider boundary conditions, such as comparing the suction change at the edge of a covered area and the middle of the covered area, Figure 4-19, or using moisture barriers, Figure 4-20. Calibrated using data collected from ten sites located in Texas within three different climatic regions, the model is as follows:

$$\frac{VM_{2D}}{VM_{1D}} = \xi_1 \exp\left(\left(\xi_2 \frac{d}{D}\right)^{\xi_3}\right) \tag{4-39}$$

Where, $VM_{2D}$ is the two-dimensional vertical movement from the FLODEF program, $VM_{1D}$ is the one-dimensional vertical movement from the MOPREC program, d is the distance from the center of the pavement to the point where the vertical movement needs to be calculated in m, D is half width of the pavement in m, and $\xi_1$, $\xi_2$ ,$\xi_3$ are regression coefficients.

For pavement width less than 18.0 m:

$$\begin{aligned}\xi_1 &= 0.0561 + 1.5872\left(d_{am}\right) + 0.1244\left(S_m\right) - 0.1936\ln\left(D\right) \\ &-0.0007139\left(VM_{1D}S_m\right) - 0.1443\left(D_b d_{am}\right)\end{aligned} \tag{4-40}$$

$$\begin{aligned}\xi_2 &= -0.068 + 0.09134\left(S_m\right) - 0.101\left(D_b\right) - 0.000188\left(TMI^2\right) + 0.321\ln\left(D\right) \\ &+0.000153\left(VM_{1D}S_m\right) + 0.000706\left(VM_{1D}D_b\right)\end{aligned} \tag{4-41}$$

$$\xi_3 = \exp\left[\begin{aligned}&1.8061 - 0.4397\left(S_m\right) + 0.4711\ln\left(D\right) + 0.08855\left(D_b{}^2\right) \\ &-0.000143\left(VM_{1D}TMI\right) + 0.003022\left(VM_{1D}D_b\right) - 1.2592\left(D_b d_{am}\right)\end{aligned}\right] \tag{4-42}$$

For pavement width greater than 22.0 m:

$$\xi_1 = 0.376 + 0.4141(d_{am}) + 0.04078(S_m) - 0.0924(D_b) \\ -0.00426(VM_{1D}S_m) - 0.02584(D_b d_{am}) \quad (4\text{-}43)$$

$$\xi_2 = -0.068 + 0.09134(S_m) - 0.101(D_b) - 0.000188(TMI^2) + 0.321\ln(D) \\ +0.000153(VM_{1D}S_m) + 0.000706(VM_{1D}D_b) \quad (4\text{-}44)$$

$$\xi_3 = \exp\left[\begin{matrix} 3.5562 - 0.8125(S_m) + 0.3707\ln(D) + 0.05649(D_b^2) \\ -0.000306(VM_{1D}TMI) - 1.6175(VM_{1D}D_b) - 0.4207(D_b d_{am}) \end{matrix}\right] \quad (4\text{-}45)$$

Where, $VM_{1D}$ is the vertical movement from 1-D program in mm, $D_b$ is the depth of barrier in m, $d_{am}$ is the depth of available moisture in m, D is half width of the pavement in m, $S_m$ is the mean suction at site in pF, and TMI is the Thornthwaite Moisture Index.

For pavement widths between 18.0 m and 22.0 m:

$$\xi = \frac{\left[\xi_{18}(22 - D) + \xi_{22}(D - 18)\right]}{4} \quad (4\text{-}46)$$

Where, $\xi$ is the parameter $\xi_1$ ,$\xi_2$ or $\xi_3$ for a pavement width of D, $\xi_{18}$ is the parameter $\xi_1$ ,$\xi_2$ or $\xi_3$ estimated from the equations for the pavement widths less than 18.0 m, and $\xi_{22}$ is the parameter $\xi_1$ ,$\xi_2$ or $\xi_3$ estimated from the equations for the pavement widths less than 22.0 m.

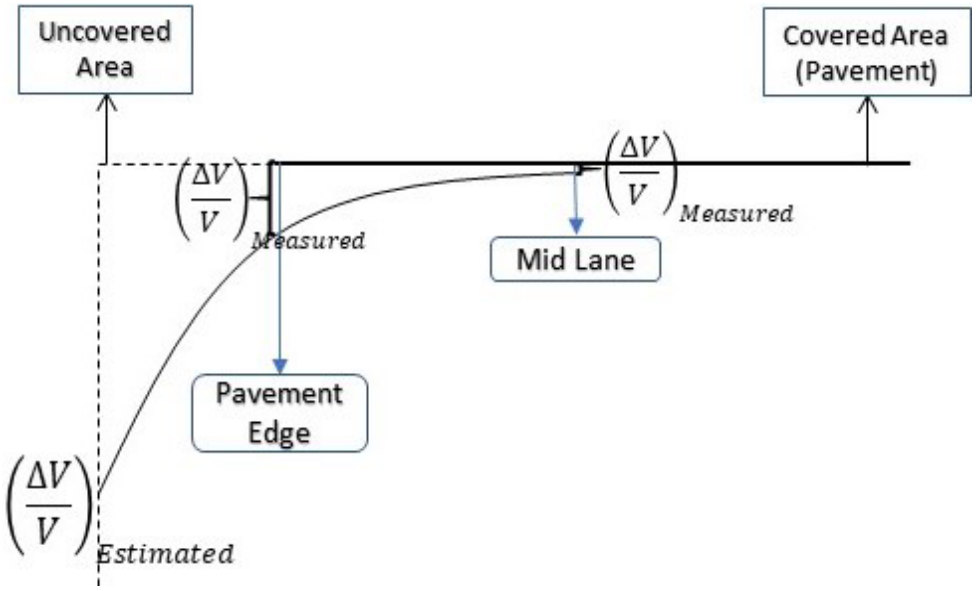


**Figure 4-19 Volume Change Due to Change in Suction in Uncovered Area Compared to Different Locations under Covered Area**

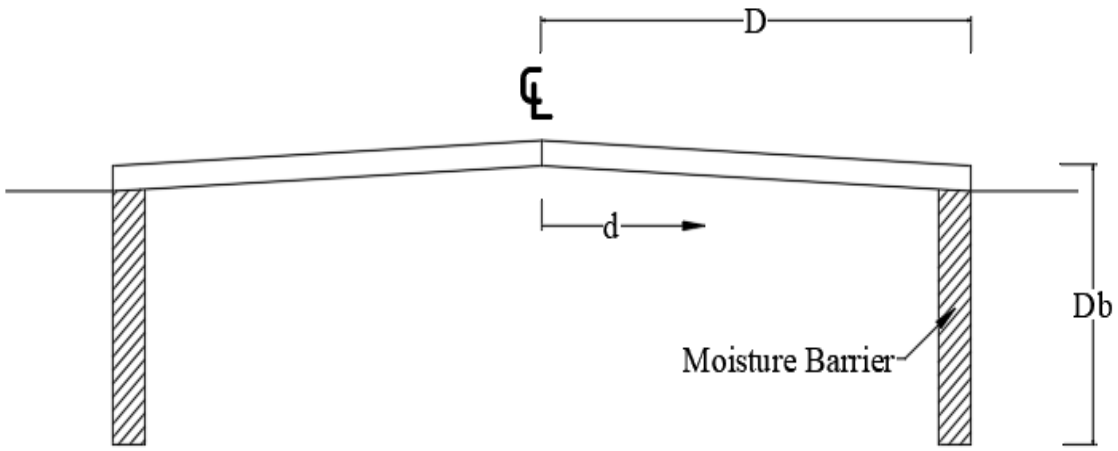


**Figure 4-20 Typical Cross-Section of a Pavement with Vertical Moisture Barriers (Jayatilaka, 1999)**

Lytton describes the depth of available moisture as the "maximum depth of the moisture that may be stored within the rooting depth of the soil profile." (Jayatilaka, 1992). This definition was expanded upon by Gay in 1994:

> "The depth of available moisture is the maximum depth of moisture available for use by transpiring vegetation, which is assumed to be stored within the rooting depth of the soil profile. This depth is dependent on the type and texture of the soil and the rooting depth; it is not dependent on the type of vegetation. It therefore represents the maximum depth of moisture that is lost from a soil during a transition from its wet state at field capacity to its dry state at the root potential (pF 4.2 - 4.5) of resident vegetation. Typical values for this depth have been reported to be between 5 cm and 20 cm (Thornthwaite 1948, Penman 1963); however, values as high as 27 cm have been reported for heavy clays at sites in Texas (Richardson and Ritchie 1973) and the Netherlands (Bouma and de Laat 1981)."

Gay (1994) also states that the depth of available moisture can be determined numerically by integrating a soil water characteristic curve (SWCC), over the root depth zone, between the saturation moisture content and the residual moisture content. Jayatilaka (1999) expresses the simplified triangular integration used to determine the depth of available moisture.

Gay (1994) and Jayatilaka (1999) state that if the soil-specific residual moisture content is unknown, the wilting point of vegetation (4.2 pF) or the air-dried state (5.7 pF) can be used depending on the general field conditions.

### *4.5.1. Effect of Moisture Barriers on SSVC Estimations*

The depth of available moisture is a parameter used to determine the effect of vertical moisture barriers used in pavement design. In order to determine the sensitivity of the depth of available moisture parameter with regards to vertical moisture barriers, the empirical relationship between 1D volume change and 2D (lateral) volume change must first be understood.

The prediction of the vertical movement on expansive soils with the inclusion of vertical moisture barriers as a special provision will be based on previous studies reported in the literature. Jayatilaka (1999) suggested a regression model to estimate the relationship between one-dimensional and two-dimensional vertical movement including the effect of vertical moisture barrier depth, using the two programs MOPREC and FLODEF developed by Gay (1994). The one-

dimensional model was based on the soil deformation model proposed by Lytton (1977). The regression model was calibrated using data collected from ten sites located in Texas within three different climatic regions.

A brief description of the required input parameters used in this model are shown in Table 4-3. All the needed parameters are available either as part of the AASHTOWare ME Pavement design procedure (i.e., pavement geometry) or from the one-dimensional model results from this project. Therefore, no additional parameters will be needed to implement the model.

**Table 4-3 Input Parameters Used in the Vertical Moisture Barrier Model**

| Input Parameter | Description |
|---|---|
| $VM_{1D}$ (mm) | Maximum vertical movement (sum of swell and shrink) |
| $D_b$ (m) | Depth of vertical moisture barrier |
| $d_{am}$ (m) | Depth of available moisture |
| $S_m$ (pF) | Mean suction |
| TMI | Thornthwaite moisture index |
| 2D (m) | Pavement width |
| d (m) | Horizontal distance from the center of pavement to point of interest |

### *4.5.2. Sensitivity Analysis of 2D SSVC Estimation*

A sensitivity analysis was conducted to recognize the most critical parameters of the 2D moisture barrier model. Fixed input values of 100 mm of maximum vertical movement, 0.3 m of depth of available moisture, 3.5 pF of mean suction and 12 m of pavement width were used. Input varied in the analysis included TMI from -40 to 40; the depth of the vertical moisture barrier from 0 to 4 meters; and the mean suction value from 0 to 4 pF. These variables were compared and plotted against a normalized vertical movement. Note that the pavement edge is located at a normalized distance of one (d/D =1). The results are presented in Figure 4-21 through Figure 4-23 below, show high sensitivity of the model to the three variables analyzed: TMI, moisture barrier depth and to the mean suction value.

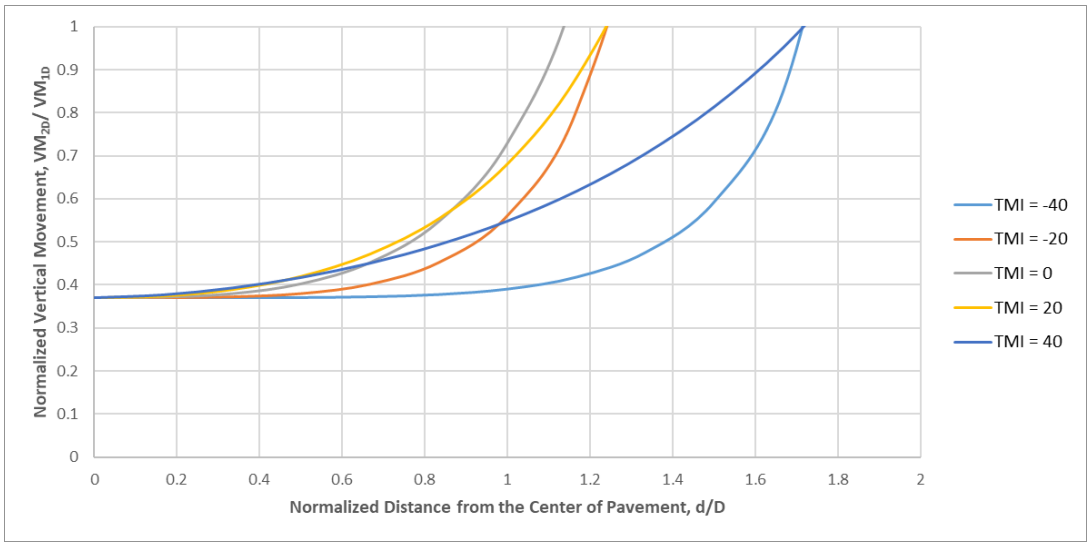


**Figure 4-21 Normalized Vertical Movement as a Function of TMI**

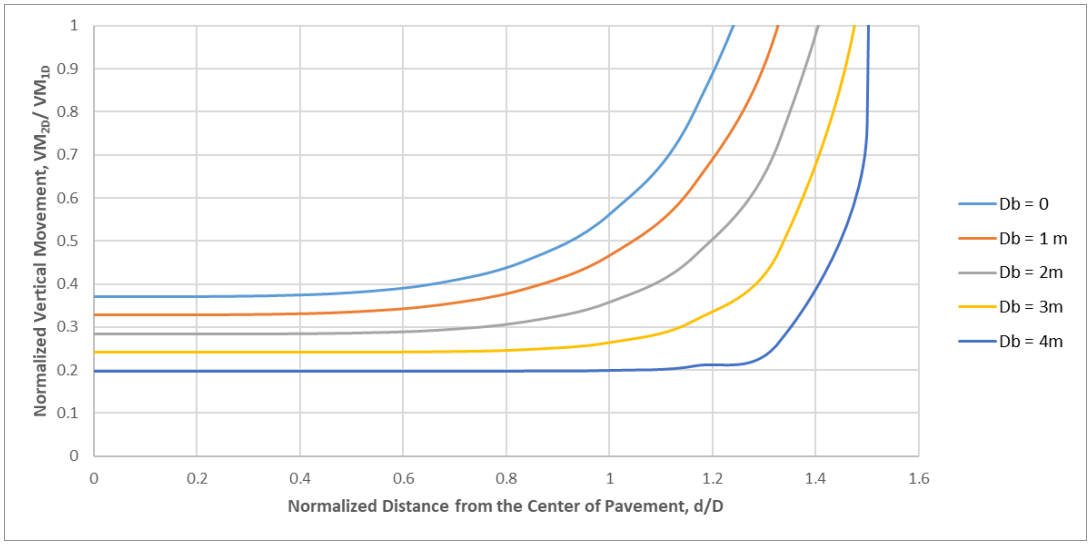


**Figure 4-22 Normalized Vertical Movement as a Function of Depth of Vertical Moisture Barrier**

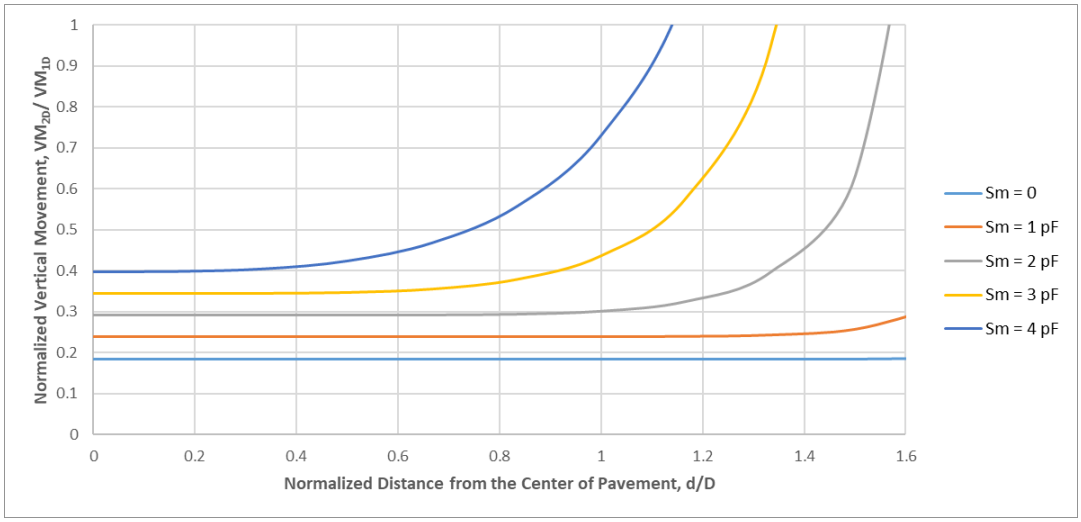


**Figure 4-23 Normalized Vertical Movement as a Function of Mean Suction**

The normalized vertical movement at the edge of the pavement is shown in Figure 4-24 and Figure 4-25 for different TMIs and Moisture barrier depths, respectively.

The research team is confident that this model will be extremely useful to 1) assess the vertical movement prediction away from the edge and towards the center of the pavement with and without moisture barriers; 2) as a surrogate path to calibration of the 1-D swelling predictions; and 3) to optimize design parameters.

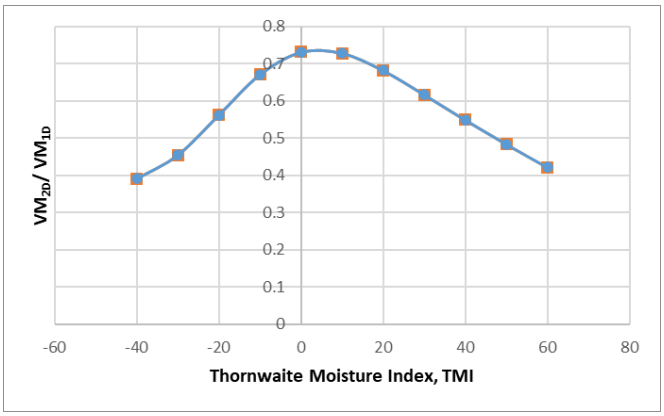


**Figure 4-24 Normalized Vertical Movement at Different Thornthwaite Moisture Index at the Edge of the Pavement**

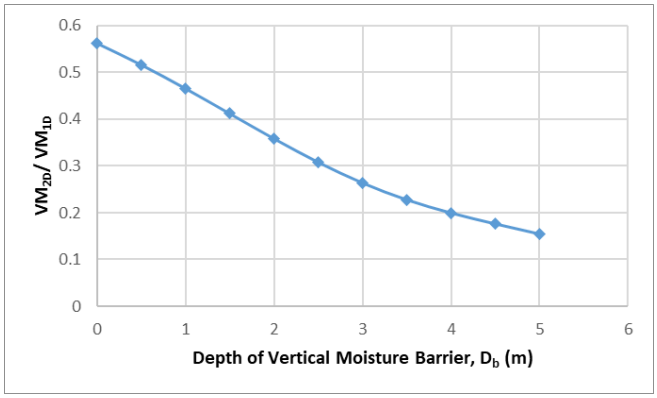


**Figure 4-25 Normalized Vertical Movement for Different Depths of Vertical Moisture Barriers at the Edge of the Pavement**

### *4.5.3. Sensitivity of the Depth of Available Moisture Parameter*

Note that Gay (1994) and Jayatilaka (1992, 1999) observed that the depth of available moisture typically does not exceed 30 cm. Therefore, the first analysis performed varied the depth of available moisture from 5 cm to 50 cm. The following table, Table 4-4, summarizes the necessary parameters used in the model. Note that only the depth of available moisture was varied; all other parameters were kept constant.

**Table 4-4 Input Parameters Used in the Vertical Moisture Barrier Model**

| Input Parameter | Value |
|---|---|
| $VM_{1D}$ (mm) | 50 mm |
| $D_b$ (m) | 0.9 m |
| $d_{am}$ (m) | variable |
| $S_m$ (pF) | 4.45 pF |
| TMI | -46.5 |
| 2D (m) | 18 m |
| d (m) | 9 m (pavement edge) |

The following figure, Figure 4-26, represents the sensitivity of the volume change at the edge of the pavement (d/D = 1) to the depth of available moisture parameter within the range of 5 to 50 cm.

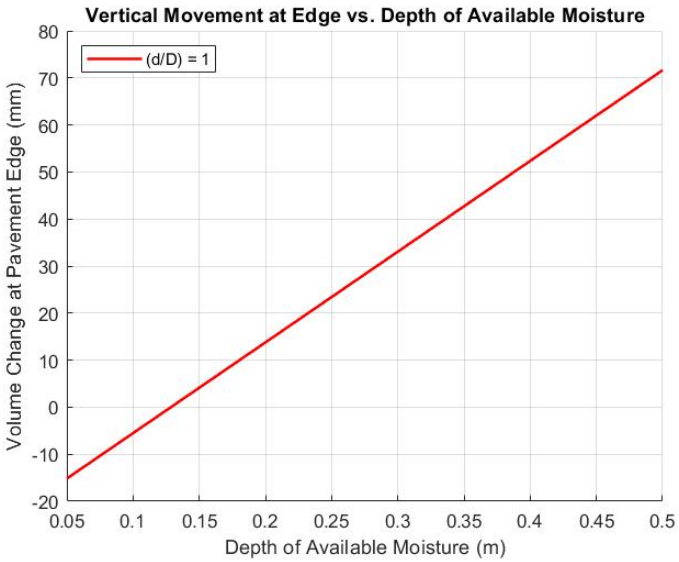


**Figure 4-26 Vertical Movement at Edge vs. Depth of Available Moisture with (d/D) = 1**

Note that empirical relationship results in negative volume change values (i.e. shrinkage) when the depth of available moisture is below approximately 12 cm (for this specific scenario). It is also important to note that the maximum vertical movement ($VM_{1D}$) of 50 mm is exceeded at the pavements edge once the depth of available moisture reaches approximately 39 cm. Based on the work on Jayatilaka (1999) and previous sensitivity analyses performed as part of this study, the lateral location of the maximum vertical movement ($VM_{1D}$) is typically outside the edge of the pavement and is affected by the TMI, mean suction, and depth of the vertical moisture barrier. Therefore, the volume change at the edge of the pavement is expected to be less than the maximum potential vertical movement value which would require the depth of available moisture to be less than 39 cm (for this specific scenario). This outcome agrees with observed depths of available moisture by Lytton (Jayatilaka 1992, 1999; Gay, 1994).

To ensure that the lateral location chosen for the sensitivity analysis above (pavement edge) did not affect the results, the same sensitivity analysis was performed with the location varying from the center of the pavement (d/D = 0) to a distance equal to half the width of the pavement away from the edge (d/D = 2).

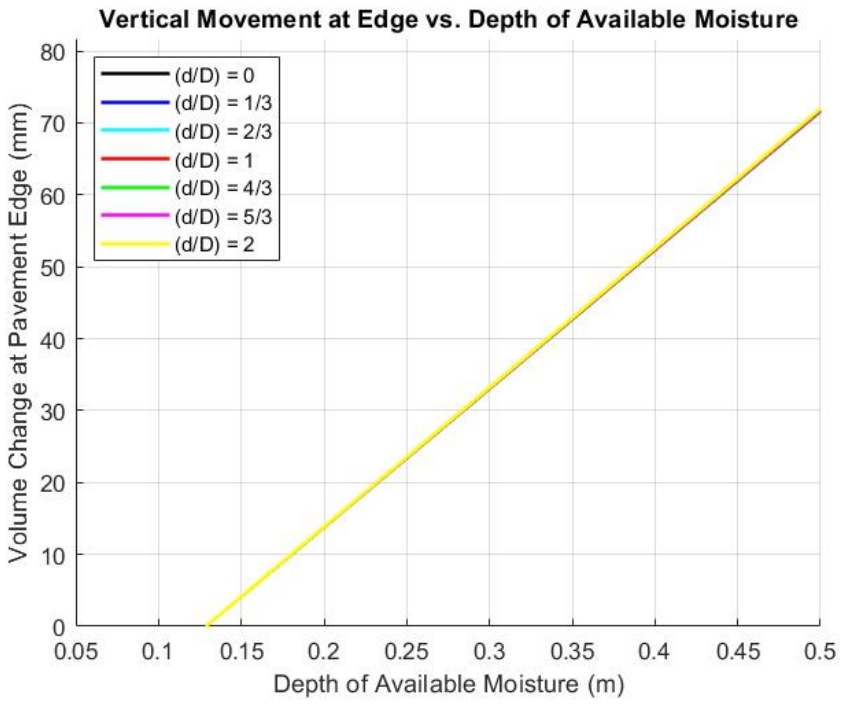


**Figure 4-27 Vertical Movement at Edge vs. Depth of Available Moisture with Varying Ratios of (d/D)**

It is clear from Figure 4-27 that the location chosen had no effect on the sensitivity analyses of the depth of available moisture. The effect of the depth of available moisture on the estimation of the volume change is insensitive to the lateral location within pavement profile.

The concept of the depth of available moisture can be confused with the depth of the active zone and the depth to equilibrium/stable suction. It is important to note that the depth of available moisture, as defined by Gay (1994) and Jayatilaka (1992, 1999), is not equivalent to the depth of stable suction, as defined by Vann (2019). To determine if the result of using the depth to stable suction (Vann, 2019) in place of depth of available moisture in the empirical estimation of the lateral heave reduction due to the presence of vertical moisture barriers, the previous analysis was performed a second time with an increased range of the depth of available moisture from 0.05 m (5 cm) to 4.5 m. The 4.5 m value represents an upper limit of the depth to stable suction observed by Cuzme (2018) and Vann (2019). Figure 4-28 represents the sensitivity of the Depth of Available Moisture parameter within the range of 0.05 m to 4.5 m.

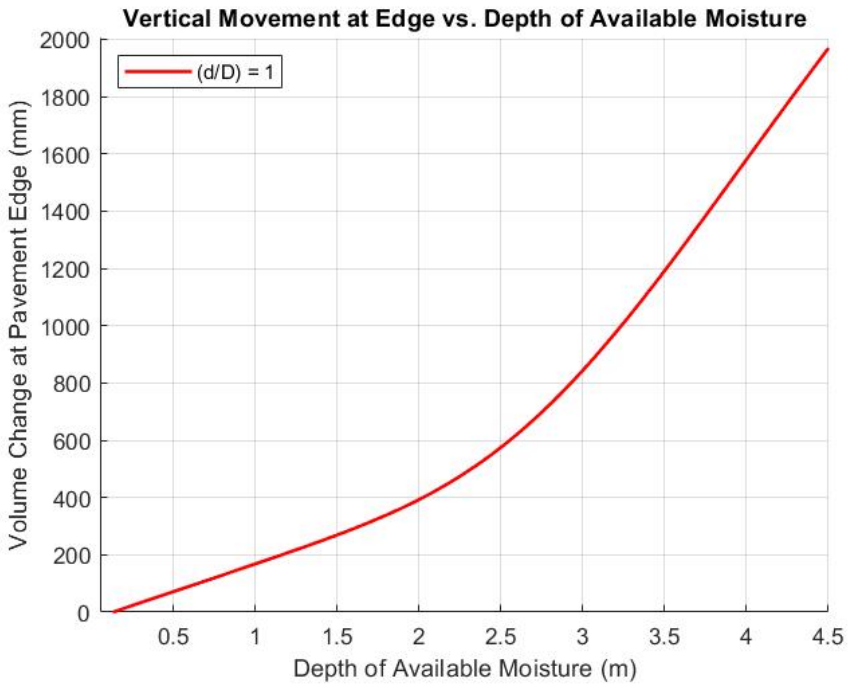


**Figure 4-28 Vertical Movement at Edge vs. Depth of Available Moisture with (d/D) = 1**

Once again, the results indicate that the magnitude of the volume change at the pavements edge is highly sensitive to the depth of available moisture parameter. If the depth to stable suction is used in-place of the depth of available moisture parameter in the analysis, the estimated volume change at the edge of the pavement will be significantly greater than the initial input of the maximum vertical movement ($VM_{1D}$ = 50 mm was used in the analysis).

In summary, it has been observed that the location of the maximum vertical movement is directly affected by the depth of available moisture, provided all other parameters remain constant.

### *4.5.4. Back Calculation of the Depth of Available Moisture*

As previously discussed, the depth of available moisture is determined from the SWCC of the soil within the root zone and knowledge of the depth of the root zone. SWCC data from all soil types is readily available and is already incorporated in the current AASHTOware software. However, data on the depth of the root zone if not readily available and may require site specific knowledge of the landscape adjacent to the roadway, which is subject to change as part of the roadway construction.

In order to eliminate the uncertainty associated with the root depth, the depth of available moisture parameter can be determined numerically if the location of the maximum vertical movement is known or estimated during the design stage. For example, a conservative assumption can be made that the maximum vertical movement will occur at the pavement edge regardless of when no vertical moisture barrier is present.

Once the location of the maximum vertical movement is assumed, an iterative calculation equivalent to the sensitivity analysis performed previously can be conducted in order to determine the depth of available moisture required for that scenario.

Table 4-5 summarizes an example scenario of a two-lane roadway with high-volume change soil, in a semi-arid climate, and variable vertical moisture barrier depth.

**Table 4-5 Input Parameters Used in the Example Vertical Moisture Barrier Model.**

| Input Parameter | Value | Comments |
|---|---|---|
| $VM_{1D}$ (mm) | 140 mm | approximately 5.5 inches |
| $D_b$ (m) | (0, 0.5, 1, 1.5, 2, 2.5, 3) m | Typical range or depths |
| $d_{am}$ (m) | Back calculated | Based on selected location of VM_1D |
| $S_m$ (pF) | 4 pF | Per Vann (2019) with TMI = 10 |
| TMI | 10 | semi-arid climate |
| 2D (m) | 19 m | two-lane road |

Figure 4-29 presents the results of the volume change at the pavement edge based on the depth of available moisture with no vertical moisture barrier.

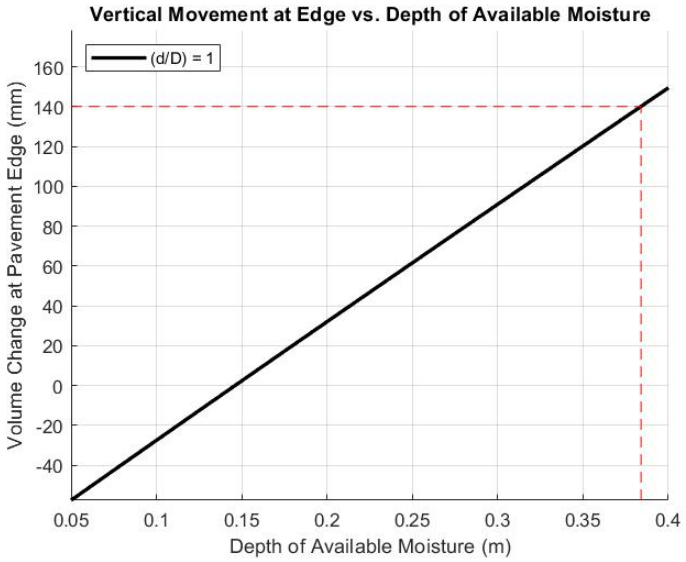


**Figure 4-29 Vertical Movement at Edge vs. Depth of Available Moisture with d/D = 1**

The red dashed lines on Figure 4-29 indicate the expected maximum vertical movement at the pavement edge when there is no moisture barrier ($VM_{1D}$) and the corresponding depth of available moisture.

The reduction in soil volume change due only to the pavement cover (no moisture barrier) can now be modeled using the moisture barrier factor (MBF) approach. Figure 4-30 represents the soil volume change due to the pavement covering alone.

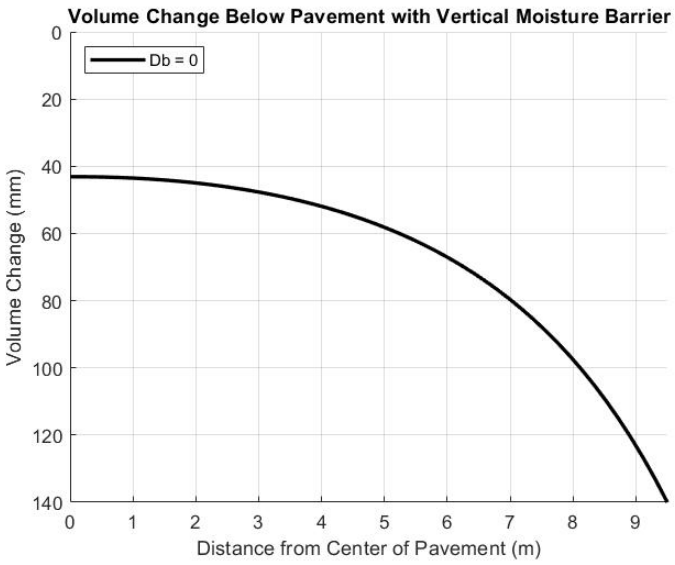


**Figure 4-30 Volume Change Below Pavement with Vertical Moisture Barrier with Db=0**

Note that volume changed is still estimated to occur at the center of the pavement for the given scenario.

The results above are commonly normalized by the maximum vertical movement and the pavement width as shown in Figure 4-31.

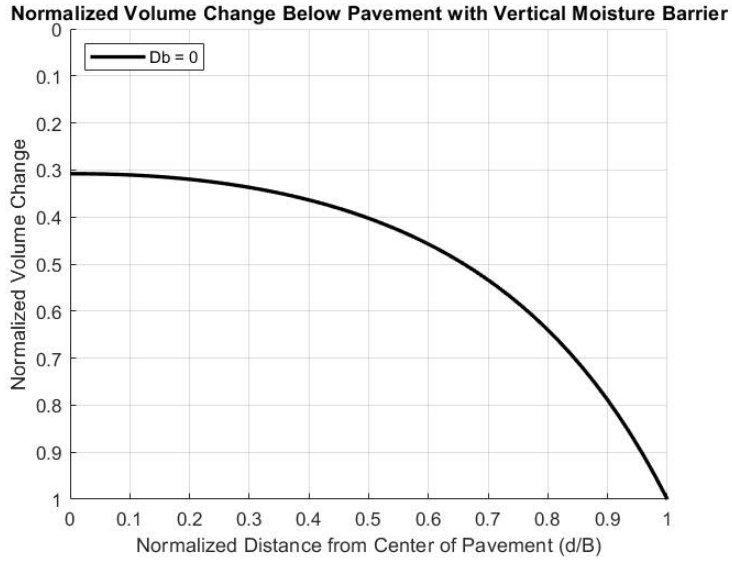


**Figure 4-31 Normalized Volume Change Below Pavement with Vertical Moisture Barrier**

By presenting the results in this manner, the percentage of the volume change reduction due to the pavement covering can be obtained from Figure 4-31 For this example, the covering from the pavement, without the presence of a vertical moisture barrier, results in approximately 30% of the maximum vertical movement occur at the edge of the pavement.

The effect of the depth of the vertical moisture barrier can now be determined using the back-calculated depth of available moisture and the parameters summarized in the table above. Figure 4-32 and Figure 4-33 present the raw and normalized results of the analysis.

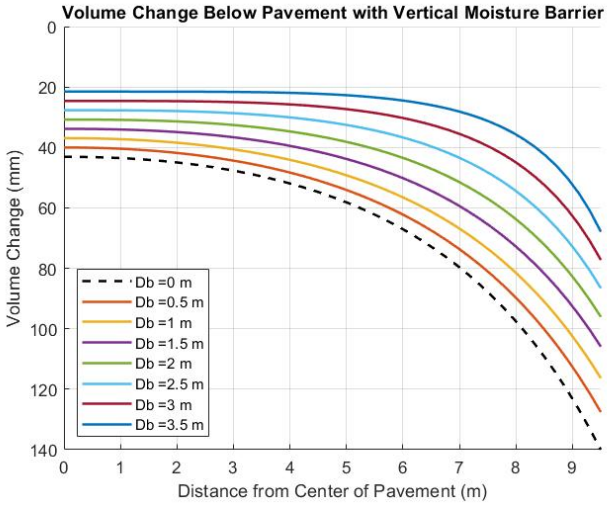


**Figure 4-32 Volume Change Below Pavement with Vertical Moisture Barrier**

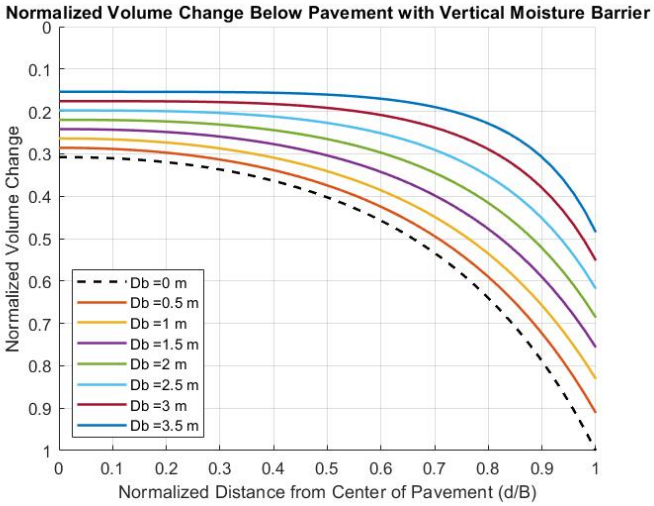


**Figure 4-33 Normalized Volume Change Below Pavement with Vertical Moisture Barrier**

Note that the estimated depth of stable suction (seasonal moisture fluctuation), for a site with a long term TMI = 10, is approximately 1.7 m (Vann, 2019). The results above indicate that a moisture barrier depth greater than the depth of stable suction (2 m) still results in vertical movements near the center of the pavement that are approximately 20% of the expected maximum vertical movement at the edge of the pavement when no barrier exists.

## 4.6. References


*AASHTO Guide for Design of Pavement Structures*. (1993). American Association of State Highway and Transportation Officials.

Aitchison, G.D. (1970). Soil aridity during occasional drought in South-Eastern Australia. *Proceedings of the Symposium on Soils & Earth Structures in Arid Climates.* Australian Geomechanics Society, May. (pp.93-97). Adelaide.

AITCHISON, G. D. & RICHARDS, B. G. (1965). A Broad scale Study of Moisture Conditions in Pavement Subgrades throughout Australia. Part 1 - 4. Butterworths, Sydney.

Aldrich Jr, P. Harl, and H. M. Paynter. (1953). *Analytical Studies of Freezing and Thawing of Soils*, *Technical Report No. 42*, Arctic Construction and Frost Effects Laboratory, New England Division U.S. Army Corps of Engineers, Boston, MA, U.S. Arctic Construction and Frost Effects Lab Boston Ma.

Alonso, E. E., Gens, A., & Josa, A. (1990). A constitutive model for partially saturated soils. *Géotechnique*, 40(3), 405-430.

Al-Shamrani, M.A. & Al-Mhaidib, A.I. (1999) Prediction of potential vertical swell of expansive soils using a triaxial stress path cell. *Quarterly Journal of Engineering Geology & Hydrogeology,* 32(1). 45-54.

Amer, Omar Mohamed Ibrahim. (2016). *Determining Suction Compression Index of Expansive Soils Based on Non-Linear Suction-Volumetric Strain Relationship*. Oklahoma State University.

AS2870-1996 *Residential Slabs & Footings.* (1996). Construction Standards Australia. Homebush, NSW, Australia.

AS2870-2011 *Residential Slabs & Footings.* (2011). Construction Standards Australia. Homebush, NSW, Australia.

Asphalt Institute (1982). Thickness Design - Asphalt Pavements for Highways & Streets. Manual Series No. 1, Asphalt Institute, Lexington, KY.

Baladi, G. Y., & Rajaei, P. (2015). *Predictive modeling of freezing and thawing of frost susceptible soils (No. RC-1619)*. Michigan State University, Department of Civil & Environmental Engineering.

Baltzer, S., H. J. Ertman-Larson, E. O. Lukanen, and R. N. Stubstad. (1994). Prediction of AC Mat Temperature for Routine Load/Deflection Measurements. *Proceedings, Fourth International Conference on Bearing Capacity of Roads and Airfields*, Volume 1. Minnesota Department of Transportation, pp. 401-412.

Basma, A. A., Al-Homoud, A. S. & Malkawi, A. I. (2000). Swelling-shrinkage behaviour of natural expansive clays. Appl. Clay Sci., 11: 211-227.

Basma. A. A. T I. Al-Suleiman (1991) Climatic Consideration in New AASHTO Flexible Pavement Design. *Journal of Transportation Engineering.* Volume 117. No 2. pp 210 to 223

Biot, M. A. (1941). General theory of three-dimensional consolidation. *Journal of applied physics*, 12(2), 155-164.

Biot, M. A., & Willis, D. G. (1957). The elastic coefficients of the theory of consolidation. *J. appl. Mech*, 15, 594-601.

Briaud, J., Zhang, X., & Moon, S. (2003). Shrink Test–Water Content Method for Shrink & Swell Predictions. *Journal of Geotechnical & Geoenvironmental Engineering, ASCE, Vol. 129, No.7*, 590–600.

Brownell, D. H., Garg, S. K., & Pritchett, J. W. (1977). Governing equations for geothermal reservoirs. *Water Resources Research*, 13(6), 929-934.

Bulut, R. (2001). "Finite Element Method Analysis of Slabs on Elastic Half Space Expansive Soil Foundations", Ph.D. Dissertation, Texas A&M University, College

Station, Texas, USA.Covar, A. and Lytton, R. (2001). "Estimating Soil Swelling Behavior Using Soil Classification Properties", *ASCE Civil Engineering Conference*, GSP 115, pp. 44-63.

Cameron, D. (2001). The extent of soil desiccation near trees in a semi-arid environment. *Geotechnical & Geological Engineering*, 19(3), 357-370.

Chan, I. & Mostyn, G. (2008). Climate Factors for AS2870 for the metropolitan Sydney area, *Australian*

*Geomechanics, Vol. 43, no.1,* (pp 17-28).

Chan, I. & Mostyn, G. (2009) Climatic factors for AS2870 for New South Wales. *Australian Geomechanics. Vol. 44, No. 2,* (pp 41- 46).

Chen, F. H. (1975). *Foundations on Expansive Soils*. Elsevier Scientific Pub. Co., Amsterdam, New York, NY.

Chen, F.H. (1988). *Foundations on Expansive Soils, 2nd ed.*: 463. Amsterdam: Elsevier.

Chisholm, R. A., and W. A. Phang. (1983). "Measurement and Prediction of Frost Penetration in Highway", Transportation Research Record: Journal of Transportation Research Board, No 918, Transportation Research Board of the National Academies, Washington D.C., pp. 1-10.

Coleman, J. D. (1965). "Geology, Climate and Vegetation as Factors Affecting Soil Moisture." *Moisture Equilibria and Moisture Changes in Soils beneath Covered Areas,* A Symposium in Print, Australia Butterworths, 93-99.

Covar, A.P. & Lytton, R.L. (2001). Estimating Soil Swelling Behavior Using Soil Classification Properties. *Geotechnical Special Publication No. 115, ASCE, Houston, Texas,* (pp 44-63).

Coussy, O. (2005). Poromechanics of freezing materials. *Journal of the Mechanics and Physics of Solids*, 53(8), 1689-1718.

Coussy, O., & Monteiro, P. (2007). Unsaturated poroelasticity for crystallization in pores. *Computers and geotechnics*, 34(4), 279-290.

Cuzme, Alan J. (2018). "Estimating Expansive Soil Field Suction Profiles Using a Soil Suction Surrogate." *Arizona State University*.

De Bruijin, C. M. A. (1961). Swelling characteristics of a transported soil profile at Leeuh of Vereeniging (Transvaal). *Proc. 5th Int. Conf. Soil Mech. Found. Eng.* 1: 43-49.

De Bruijin, C. M. A. (1965). Some observations on soil moisture conditions beneath & adjacent to tarred roads & other surface treatments in South Africa. *Moisture Equilibrium & Moisture Changes Beneath Covered Areas.* (pp. 135-142). Butterworths, Australia.

Dhowian, A. W. (1990). Field performance of expansive shale formation, *Journal of King Abdulaziz University (Engineering Sciences)*, 2: 165-82.

Dhowian, A.W., Erol, A.0. & Youssef, A. (1990). *Evaluation of Expansive Soils & Foundation Methodology in the Kingdom Saudi Arabia*.

Dolinar, B., & Škrabl, S. (2013) Atterberg limits in relation to other properties of fine-grained soils. *Acta Geotechnica Slovenica*, 2, 1-13.

Doré, G., Konrad, J. M., & Roy, M. (1997). Role of deicing salt in pavement deterioration by frost action. *Transportation Research Record: Journal of the Transportation Research Board*, (1596), 70-75.

Doré, G., Konrad, J. M., & Roy, M. (1999). Deterioration model for pavements in frost conditions. *Transportation Research Record: Journal of the Transportation Research Board*, (1655), 110-117.

Doré, G., Flamand, M., & Tighe, S. (2001). Prediction of winter roughness based on analysis of subgrade soil variability. *Transportation Research Record: Journal of the Transportation Research Board*, (1755), 90-96.

Doré, G. (2002). Cold region pavement. *Journal of Glaciology and Geocryology*, 24(5), 593-600.

Doré, G., & Zubeck, H. (2009). Cold regions pavement engineering. New-York: McGraw-Hill/ASCE press.

Duquennoi, C. M. Fremond, and M. Levy. 1989. Modelling of thermal soil behavior. P. 895-915. In H. Rathmayer (ed.) Frost in geotechnical engineering, Int. Symp., Saariselk, Finland. 13-15 Mar. 1989. VTT Symp. 94. Valtion Teknillinen Tutkimuskeskus, Espoo, Finland.

Erol, A. O., Dhowian A. & Youssef, A. (1987). Assessment of oedometer methods for heave prediction. *Proceedings of 6th International Conference on Expansive Soils, Technical Session III*. pp. 99-105.

Federal Highway Administration. (June 2000). Temperature Predictions and Adjustment Factors for Asphalt Pavement. Publication No. FHWA-RD-98-085, McLean, VA.

Fernando, E. G., Liu, W., & Ryu, D. (2001). *Development of a procedure for temperature correction of backcalculated AC modulus* (No. FHWA/TX-02/1863-1,). Texas Transportation Institute, Texas A & M University System.

Fityus, S.G., P.F. Walsh, & P.W. Kleeman. (1998). The influence of climate as expressed by the Thornthwaite index on the design of depth of moisture change of clay soils in the Hunter Valley. Conference on Geotechnical Engineering & Engineering Geology in the Hunter Valley. (pp. 251-265) Springwood, Australia.

Fityus, S., & Buzzi, O. (2008). On the use of the Thornthwaite moisture index to infer depths of seasonal moisture change. Australian Geomechanics 43 (4): 69-76.

Fityus, S. & Smith, D. W. (1998). A simple model for the prediction of free surface movements in swelling clay profiles. Proceedings of the 2nd International Conference on Unsaturated Soils. (pp. 473-478). Beijing, China.

Fityus, S., Smith, D.W., & Allman, M.A. (2004). Expansive Soil Test Site Near Newcastle. Journal of Geotechnical and Geoenvironmental Engineering, ASCE, 130(7): 686-695.

Fityus, S. & Smith, D.W. (2004). The Development of a Residual Soil Profile from a Mudstone in a Temperate Climate. *Engineering Geology*, 74, 39-56.

Fredlund, D. G., Morgenstern, N. R., and Widger, R. A. (1978). The Shear Strength of Unsaturated Soils. *Canadian Geotechnical Journal*, 15(3), 313-321.

Fredlund, D. G., Hasan, J. U., & Filson, H. (1980). The prediction of total heave. *Proceedings 4th International Conference on Expansive Soils*. (pp. 1-11) Denver, Colorado.

Fredlund, D. and Rahardjo, H. (1993). Soil Mechanics for Unsaturated Soils. New York, NY, USA: John Wiley and Sons, Inc.

Fredlund, D.G., A. Xing, and S. Huang. (1994). Predicting the permeability function for unsaturated soils using the soil-water characteristic curve. *Can. Geotech. J.* 31 pp. 533–546. doi:10.1139/t94-062.

Fredlund, D. G., et al. (2012). *Unsaturated Soil Mechanics in Engineering Practice*. Wiley.

Fremond, M., and M. Mikkola. (1991). Thermomechanical modeling of freezing soil. p. 17-24. In X. Yu and C. Wang (ed.) Ground freezing '91: Proc. Int. Symposium on Ground Freezing, 6th, Beijing. 10-12 Sept. 1991. A.A. Balkema, Rotterdam, the Netherlands.

Gibbs, H.J. (1973) Use of a consolidometer for measuring expansion potential of soils. *Proc. Workshop Expansive Clays & Shales in Highway Design & Construction*. *Univ. Wyoming, Laramie, May, 1*: 206-213.

Gilpin, R. (1980). A model for the prediction of ice lensing and frost heave in soils. *Water Resources Research*, 16(5), 918-930.

Guide for Mechanistic-Empirical Design of New and Rehabilitated Pavement Structures Appendix BB: Design Reliability. 2003

Guymon, G. L., & Luthin, J. N. (1974). A coupled heat and moisture transport model for arctic soils. *Water Resources Research*, 10(5), 995-1001.

Guymon, G.L., Berg, R.L., and Johnston, T.C., *Mathematical Model of Frost Heave and Thaw Settlement in Pavement, Report*: U.S. Army Cold Regions Research and Engineering Laboratory, 1986.

Hamberg, D.J. & Nelson, J.D. (1984). Prediction of floor slab heave. *Proceedings of 5th International Conference on Expansive Soils*. (pp. 137-140) Adelaide, South Australia.

Han, S. J., and Goodings, D.J. (2006). "Practical model of frost heave in clay." Journal of geotechnical and geoenvironmental engineering 132, no. 1, pp. 92-101.

Hansson, K., Šimůnek, J., Mizoguchi, M., Lundin, L. C., & Van Genuchten, M. T. (2004). Water flow and heat transport in frozen soil. Vadose Zone Journal, 3(2), 693-704.

Harlan, R.L. (1973). Analysis of coupled heat-fluid transport in partially frozen soil. *Water Resources Research*, 9(5), 1314-1323.

Hayhoe, H. N., and Balchin, D. (1990). "Field frost heave measurement and prediction during periods of seasonal frost." Canadian Geotechnical Journal 27, no. 3, pp. 393-397.

Hoerner, T., E., Darter, I., M., Khazanovich and Titus-Glover, L., S. (2000). Improved prediction models for pcc pavement performance-related specifications. Final Report, Federal Highway Administration, Washington, DC.

Holtz, W.G. and Gibbs, H.J. (1956). Engineering Properties of Expansive Clays. *Trans. ASCE, vol. 121*, 641-663.

Holtz, W.G. (1959). Expansive Clays-Properties & Problems, in Theoretical & Practical Treatment of Expansive Soils. *1st Conf. Mech. Soils, Colorado School of Mines, Golden, Vol. 54*, No. 4, 89-117.

Houston, W.N., Mirza, M.W. and Zapata, C. E. (2006). *Environmental Effects in Pavement Mix Structure Design Systems*. Calibration & Validation of the ICM Version 2.6. *NCHRP 9-23 Final Report.* Arizona State University, Tempe, Arizona.

Houston, S. and Houston, W. (2017). A suction-oedometer method for computation of heave & remaining heave. *Proc. of the 2nd PanAm Conf. on Unsaturated Soils, Dallas, TX, Vol. 1, ASCE*.

Hromadka II, T. V. and Yen, C.C. (1986). A diffusion hydrodynamic model (DHM). *Advances in water resources*, 9(3), 118-170.

Huang, Yang H. (2004). *Pavement Analysis and Design*. Second ed., Pearson/Prentice Hall.

Jaksa, M.B., Kaggwa, W.S., Woodburn, J.A. & Sinclair, R. (2002). Influence of large gum trees on the soil suction profile in expansive soils. *Australian Geomechanics, Vol.37.* No. 1, pp. 23-33

Jame, Y. W., & Norum, D. I. (1980). Heat and mass transfer in a freezing unsaturated porous medium. *Water Resources Research*, 16(4), 811-819.

Janoo, V. C., & Berg, R. L. (1990). Thaw weakening of pavement structures in seasonal frost areas. *Transportation Research Record: Journal of the Transportation Research Board*, (1286), 217-233.

Jayatilaka, R., Gay, D., Lytton, R., &Wray, W. (1992). Effectiveness of controlling pavement roughness due to expansive clays with vertical moisture barriers. *Research Study No. 2/11-8-88-1165.* Texas Depart of Transportation, Texas Transportation Institute, & Texas Tech University, 230 p

Jennings, J. E. B., Firtu, R. A., Ralph, T. K. & Nagar, N. (1973). An improved method for predicting heave using the oedometer test. *Proc. 3rd Int. Conf. Expansive Soils*, Haifa, Israel, 2: 149-154.

Jennings, J.E., & Knight, K. (1957). The prediction of total heave from double oedometer test, In *Proceedings of Symposium on Expansive Clays*. South African Institution of Civil Engineers, Johannesburg, 13-19.

Jiji, L. M. (2009). *Heat Conduction*, Berlin: Springer.

Johnson, L.D. (1977). Evaluation of Laboratory Suction Tests for Prediction of Heave in Foundation Soils. *Tech. Reports S-77-7*, U.S. Army Engineer Waterways Experiment Station, Vicksburg, MS, 118 pp.

Johnson, L. D. & Snethen, D. R. 1978. Prediction of potential heave of swelling soils. *Geotechnical Testing Journal, 1*(3): 117-124.

Karunarathne, A.M.A.N., E.F. Gad, S. Sivanerupan, & J.L. Wilson. (2016). Review of Calculation Procedures of Thornthwaite Moisture Index & Its Impact on Footing Design. *Australian Geomechanics 51* (1): 85-95.

Konrad, J. M. and Morgenstern, N. R. (1980). A mechanistic theory of ice lens formation in fine-grained soils. *Canadian Geotechnical Journal*, 17(4), 473-486.

Konrad, J.M. and Morgenstern, N.R. (1981). The segregation potential of a freezing soil. *Canadian Geotechnical Journal*, 18(4), 482-491.

Konrad, J.M. and Morgenstern, N.R. (1982a). Prediction of frost heave in the laboratory during transient freezing. *Canadian Geotechnical Journal*, 19(3), 250-259.

Konrad, J. M., & Morgenstern, N. R. (1982b). Effects of applied pressure on freezing soils. *Canadian Geotechnical Journal*, 19(4), 494-505.

Konrad, Jean-Marie. (2005). "Estimation of the segregation potential of fine-grained soils using the frost heave response of two reference soils." Canadian Geotechnical Journal 42, no. 1, pp. 38-50.

Konrad, Jean-Marie. (1999). "Frost susceptibility related to soil index properties." Canadian Geotechnical Journal 36,

no. 3, pp. 403-417.

Lee, H. C. and Wray, W. K. (1995). Techniques to Evaluate Soil Suction – A Vital Unsaturated Soil Water Variable. In Alonso, E. E. and Delage, P. (Eds.). Unsaturated Soils. Proceedings of the First International Conference on Unsaturated Soils, UNSAT'95. (pp. 615-622). Paris, France.

Li, J, Cameron, D and Ren, G (2013). Case study and back analysis of a residential building damaged by expansive soils, *Computers and Geotechnics*, vol. 56, pp. 89-99.

Li, N., Chen, B., Chen, F., & Xu, X. (2000). The coupled heat-moisture-mechanic model of the frozen soil. *Cold Regions Science and Technology*, 31(3), 199-205.

Li, N., Chen, F., Su, B., & Cheng, G. (2002). Theoretical frame of the saturated freezing soil. *Cold Regions Science and Technology*, 35(2), 73-80.

Livneh, M., Kinsky, J. and Zaslavsky, D. (1970). Correlation of Suction Curves with the Plasticity Index of Soils. Journal of Materials, JMLSA, 5(1), 209-220.

Liu, Z., Yu, X. B., Tao, J. L., & Sun, Y. (2012). Multiphysics extension to physically based analyses of pipes with emphasis on frost actions. *Journal of Zhejiang University-Science A*, 13(11), 877-887.

Lopes, D. (2006). Characterization of Victorian sites using a suction sign post shrinkage test with reference to geological & climate settings. *Australian Geomechanics Vol 41*, No 4. pp 105-110.

Lopes, D. (2007). "A Modified Shrink/Swell Test to Calculate the Instability Indices of Clays", *Australian Journal of Civil Engineering*, Institution of Engineers Australia, Vol. 3, No. 1, pp. 67-74.

LTPP InfoPave, U.S. Department of Transportation/Federal Highway Administration, https://infopave.fhwa.dot.gov/.

"LTPP Information Management System Data." (2003). Release 15.0. Version 2002.11. Primary Data Set All QC Levels, Volume 1.

Lu, L. (2010). A simple technique for estimating the 1-D heave of natural expansive soils. Master's Thesis, Department of Civil Engineering, University of Ottawa, Canada, 171 p.

Lu, N., & Likos, W. J. (2006). Suction stress characteristic curve for unsaturated soil. *Journal of geotechnical and geoenvironmental engineering*, 132(2), 131-142.

Lytton, R.L. (1977). *Foundations in Expansive Soils, in Numerical Methods in Geotechnical Engineering*, Chapter 13. (pp. 427-458). C. S. Desai & J. T. Christian (Eds.), New York: McGraw-Hill.

Lytton, R., Aubeny, C., Bulut, R. (2004). Design procedure for pavements on expansive soils. *Report 0-4518-1 Vol.1, Project Number 0-4518*, Texas Department of Transportation & the U.S. Department of Transportation Federal Highway Administration, Texas Transportation Institute, 198 p.

Lytton, R., C. Aubeny, and R. Bulut. (2005). Design Procedures for Soils on Expansive Soils: Volume 1. FHWA/TX-05/0-4518. Texas Department of Transportation.

Lytton, R. L., D. E. Pufahl, C. H. Michalak, H. S. Liang, and K. J. Dempsey. (1990). "An Integrated Model of the Climatic Effects on Pavement." Report No. FHWA-RD-90-033. Federal Highway Administration, *Texas Transportation Institute*, Texas A&M University McLean, VA.

MacKay, M. H., Hein, D. K., & Emery, J. J. (1992). Evaluation of frost action mitigation procedures for highly frost-susceptible soils. *Transportation Research Record: Journal of the Transportation Research Board*, (1362), 79-89.

McKeen, R. (1992). A model for predicting expansive soil behavior. *Proceedings of the 7th International Conference on Expansive Soils*, (pp. 1-6). Dallas, Texas.

McKeen, R.G. & Hamberg, D.J. (1981). Characterization of Expansive Soils. *Trans. Res. Rec. 790*, Trans. Res. Board, (pp. 73-78).

McKeen, R. G. and Johnson, L. D. (1990). "Climate-Controlled Soil Design Parameters for Mat Foundations". J. of Geotechnical Eng., 116(7), pp. 1073-1094.

McKeen, R. (1992). A model for predicting expansive soil behavior. *Proceedings of the 7th International Conference*

*on Expansive Soils*, (pp. 1-6). Dallas, Texas.

*Mechanistic-Empirical Pavement Design Guide: A Manual of Practice*. (2008). American Association of State Highway and Transportation Officials.

Miller, R. D. (1972). Freezing and heaving of saturated and unsaturated soils. *Highway Research Record*, (393).

Miller, R. D. (1973). Soil freezing in relation to pore water pressure and temperature. pp. 344-452. In International Conference on Permafrost, 2nd, Yakutsk, Siberia, 11-28 July 1973. Natl. Acad. Sci., Washington, DC.

Miller, R. D. (1978). Frost heaving in non-colloidal soils. In Proceeding 3rd International Conference Permafrost (pp. 707-713). National Research Council of Canada.

Miller, R. D. (1980). Freezing phenomena in soils. Applications of soil physics.

Minnesota Department of Transportation (MnDOT), (2009). "Guidelines for Seasonal Load Limit Starting and Ending Dates", Policy, Safety & Strategic Initiatives Division Technical Memorandum. No. 09-09-MAT-02.

Mitchell, P.W. (1979). The Structural Analysis of Footings on Expansive Soil. Newton: Kenneth W.G. Smith& Associates.

Mitchell, P.W. (1980). The Concepts Defining the Rate of Swell of Expansive Soils. *Proceedings of the 4th International Conference on Expansive Soils*. Denver, USA. Volume 1, pp 106-116.

Mitchell, P.W. (2008). Footing Design for Residential Type Structures in Arid Climates. *Australian Geomechanics Vol. 41*, No 4. pp 51-68.

Mitchell, P.W. (2013). Climate Change Effects on Expansive Soil Movements. *Proceedings of the 18th International Conference on Soil Mechanics and Geotechnical Engineering*. Paris, 1159-1162.

Mitchell, P.W., & Avalle, D.L. (1984). A Technique to Predict Expansive Soil Movements. *Proceedings of 5th International Conference on Expansive Soils*. Adelaide, South Australia.

Mizoguchi, M. (1990). Water heat and salt transport in freezing soil. Ph.D. diss. Univ. of Tokyo, Tokyo.

Mutou, Y., Watanabe, K., Mizoguchi, M., & Ishizaki, T. Microscopic observation of ice 718 lensing and frost heaves in glass beads. In Proceedings of the 7th International Conference 719 on Permafrost (pp. 783-787).

Nakano, Y., & Brown, J. (1971). Effect of a freezing zone of finite width on the thermal regime of soils. *Water Resources Research*, 7(5), 1226-1233.

Navy, Dept. of, Naval Facilities Engineering Command. (1971). *Design Manual-Soil Mechanics, Foundations & Earth Structures*. U. S. Naval Publications & Forms Center, NAVFAC DM-7.

Nayak, N. V. & Christensen, R. W. 1971. Swell characteristics of compacted expansive soils. *Clay & Clay Minerals. 19*(4): 251-261.

Neaupane, K. M., & Yamabe, T. (2001). A fully coupled thermo-hydro-mechanical nonlinear model for a frozen medium. *Computers and Geotechnics*, 28(8), 613-637.

Nelson, John D., and Debora J. Miller. (1992). *Expansive Soils: Problems and Practice in Foundation and Pavement Engineering*. John Wiley & Sons, Inc.

Nelson, J.D., Overton, D.D., & Durkee, D.B. (2001). Depth of Wetting & the Active Zone. *Proceedings of Expansive Clay Soils & Vegetative Influence on Shallow Foundations, October 10-13, 2001, Houston, Texas*, USA, ASCE, 95-109.

Newman, G. P., & Wilson, G. W. (1997). Heat and mass transfer in unsaturated soils during freezing. *Canadian Geotechnical Journal*, 34(1), 63-70.

Nishimura, S. A. Gens, S. Olivella, and R. J. Jardine. (2009). THM-coupled finite element analysis of frozen soil: Formulation and application. *Geotechnique* 59: 159-171. Doi: 10.1680/geot.2009.59.3.159

Nixon, John F. (1982). "Field frost heave predictions using the segregation potential concept. *Canadian Geotechnical Journal* 19, no. 4, pp. 526-529.

Nixon, J. F. (1991). Discrete ice lens theory for frost heave in soils. *Canadian Geotechnical Journal*, 28(6), 843-859.

Nobel, C. A. (1966). Swelling measurements & prediction of heave for a lacustrine clay. *Can. Geotechnical Journal 3*(1): 32-41.

Noborio, K., McInnes, K. J., & Heilman, J. L. (1996). Two-dimensional model for water, heat, and solute transport in furrow-irrigated soil: I. Theory. *Soil Science Society of America Journal*, 60(4), 1001-1009.

Olaiz, A.H.; Singhar, S.H.; Vann, J.D. & Houston, S.L. (2016). Comparison & applications of the Thornthwaite moisture index using GIS. *Proc. of the 2nd PanAm Conf. on Unsaturated Soils, Dallas, TX, Vol. 1*, ASCE

Olaiz, A.H. (2017). "Evaluation of Testing Methods for Suction-Volume Change of Natural Clay Soils." *Arizona State University*.

Oloo, S. Y. and Fredlund, D. G. (1995). Matric Suction Monitoring in an Expansive Soil Subgrade in Kenya. In Alonso, E. and Delage, P. (Eds.). Unsaturated Soils. Proceedings of the First International Conference on Unsaturated Soils, UNSAT'95 (pp. 631- 636). Paris, France.

Ongel, A., & Harvey, J. (2004). Analysis of 30 years of pavement temperatures using the enhanced integrated climate model (EICM). Pavement Research Centre.

Oswell, J. M. (2011). Pipelines in permafrost: geotechnical issues and lessons 1 2010 RM Hardy Address, 63rd Canadian Geotechnical Conference. *Canadian Geotechnical Journal*, 48(9), 1412-1431.

O'Neill, K., & Miller, R. D. (1985). Exploration of a rigid ice model of frost heave. *Water Resources Research*, 21(3), 281-296.

Perera, R W, and A Al-Rawashdeh. (2017). *Investigation of Increase in Roughness Due to Environmental Factors in Flexible Pavements Using Profile Data from Long-Term Pavement Performance Specific Pavement Studies 1 Experiment*. FHWA-HRT-17-049.

Perera, Y. Y. (2003). Moisture Equilibria beneath Paved Areas. Ph.D. Dissertation, Arizona State University, Arizona, U.S.A.

Perera, Y.Y., Zapata, C.E., Houston, W.N., and Houston, S.L. (2004a). Long-Term Moisture Conditions under Highway Pavements. In M.K. Yegian & E. Kavazanjian, (eds.), *Geotechnical Special Publication No. 126, Geotechnical Engineering for Transportation Projects*, ASCE Geo-Institute. Los Angeles, CA, Vol. 1, pp. 1132-1143. Also, *Proceedings of Geo-Trans 2004,* July 27-31. Student participation: 30%; Zapata's contribution: 30%

Perera, Y.Y., Zapata, C.E., Houston, W.N. and Houston, S.L. (2005). Prediction of the Soil-Water Characteristic Curve Based on Grain-Size Distribution and Index Properties. In E.M. Rathje (ed.), GSPs 130-142 & GRI-18; ASCE Geo-Institute and Geosynthetic Materials Association of the Industrial Fabrics Association International Geosynthetic Institute. CD-ROM.

Perko, H. A., Thompson, R. W., & Nelson, J. D. (2000). Suction Compression Index Based on CLOD Test Results. GEO-Denver (pp. 395-407). Denver, CO: ASCE.

Picornell, M. & Lytton, R. L. (1984). Modeling the heave of a heavily loaded foundation. *Proceeding of 5th International Conference on Expansive Soils.* (pp. 104-108). Adelaide, Australia.

Plagge, R., Roth, C. H., and Renger, M. (1992). A New Laboratory Method to Rapidly Determine the Unsaturated Soil Hydraulic Properties. In van Genuchten, M. Th., Leij, F. J., and Lund, L. J. (Eds.). Proceedings of the International Workshop on Indirect Methods for Estimating the Hydraulic Properties of Unsaturated Soils (pp. 653-663). Riverside, CA: University of California.

Porter, A. A. & Nelson, J. D. (1980). Strain controlled testing of soils. *Proc. 4th Int. Conf Expansive Soils, ASCE & Int. Soc. Soil Mech. Found. Eng.* (pp. 34-44). Denver, CO.

Post-Tensioning Institute. (2004). *Design of Post-Tensioned Slabs-on-Ground.* Phoenix: 3rd Edition, Post-Tensioning Institute.

Post-Tensioning Institute, (2008). *Design & construction of post-tensioned slabs-on-ground, 3rd edition*. Post Tensioning Institute, Phoenix.

Powers, T. C., & Willis, T. F. (1950). The air requirement of frost resistant concrete. *In Highway Research Board Proceedings* (Vol. 29).

Rabin, Y., & Steif, P. S. (1998). Thermal stresses in a freezing sphere and its application to cryobiology. *Journal of applied mechanics*, 65(2), 328-333.

Rada, G. R., Elkins, G. E., Henderson, B., Van Sambeek, R. J., and Lopez, Jr., A. (1994). *LTPP Seasonal Monitoring Program: Instrumentation Installation and Data Collection Guidelines.* FHWA-RD-94-110.

Ranganathan, B. V. & Satyanarayana, B. (1965). A rational method of predicting swelling potential for compacted expansive clays. *Proceedings of the 6th International Conference on Soil Mechanics & Foundation Engineering. International Society for Soil Mechanics & Geotechnical Engineering, London, 1*: 92-96.

Richards, S. J. (1965). Soil Suction Measurements with Tensiometers. In Black, C. A. (Ed.). Methods of Soil Analysis, Part 1: Physical and Mineralogical Properties, Including Statistics of Measurement and Sampling (pp. 153-163).

Ridley, A. M., and Wray, W. K. (1995) Suction Measurement: A Review of Current Theory and Practices. In Alonso, E. and Delage, P. (Eds.). Unsaturated Soils. Proceedings of the First International Conference on Unsaturated Soils, UNSAT'95 (pp. 1293-1322). Paris, France.Rosenbalm, Daniel. (2011). "Reliability Associated with the Estimation of Soil Resilient Modulus at Different Hierarchical Levels of Pavement Design." *Arizona State University*.

Rosenbalm, Daniel, and Claudia E. Zapata. (2017). "Effect of Wetting and Drying Cycles on the Behavior of Compacted Expansive Soils." *Journal of Materials in Civil Engineering*, vol. 29, no. 1, p. 04016191.

Roy, M., Crispin, J., Konrad, J. M., & Larose, G. (1992). Field study of two road sections during a freeze-thaw cycle. *Transportation Research Record: Journal of the Transportation Research Board*, (1362), 71-78

Russam, K. and J. D. Coleman. (1961) The Effect of Climatic factors on Subgrade Moisture Conditions. *Geotechnique***.** Volume XI, No. 1, pp 22 to 28.

Sampson, E., Schuster, R. L. & Budge, W. D. (1965). A method of determining swell potential of an expansive clay. *Proc. Engineering Effects of Moisture Changes in Soils. Int. Res. Eng. Conf Expansive Clay Soils*. Texas A & M Univ. Press, College Station, TX, pp. 255-275.

Sandra, Amarendra Kumar, and Ashoke Kumar Sarkar. (2013). "Development of a Model for Estimating International Roughness Index from Pavement Distresses." *International Journal of Pavement Engineering*, vol. 14, no. 8, pp. 715–724.

Schaus, L., Eng, P., Popik, M., & Eng, M. (2011). Frost heaves: a problem that continues to swell. In *2011 Conference and Exhibition of the Transportation Association of Canada. Transportation Successes: Let's Build on Them.*

Schneider, G.L. & Poor, A.R. (1974). The prediction of soil heave & swell pressures developed by an expansive clay. *Research Report, No: TR-9-74*. Construction Research Center, Univ. of Texas.

Schofield, R.K. (1935). "The pF of Water in Soil" Trans, 3rd Int. Congr. Soil Sci. (Oxford), 2, pp. 37-48.

Seed, H. B., Woodward, R.J., & Lundgren, R. (1962). Prediction of Swelling Potential for Compacted Clays. *Journal of the Soil Mech. Found. Div., ASCE, vol. 88*, no. SM4, 57-59.

Shanker, N. B., Ratnam M. V. & Rao A. S. (1987). Multi-dimensional swell behaviour of expansive clays. *Proc. 6th Int. Conf. Expansive Soils*. New Delhi, India.

Sheng, D., Axelsson, K., & Knutsson, S. (1995). Frost heave due to ice lens formation in freezing soils: 1. Theory and verification. *Hydrology Research*, 26(2), 125-146.

Singhal, S. (2010). *Expansive Soil Behavior: Property Measurement Techniques & Heave Prediction Methods.* Ph.D. Dissertation, Arizona State University, Tempe, AZ, USA

Smith, A. W. (1973). Method for determining the potential vertical rise, PVR. *Proc. Workshop Expansive Clays & Shales in Highway Design & Construction*. Univ. of Wyoming, Denver, CO, pp. 245-249.

Snethen, D. (1980). *Proceedings of the Fourth International Conference on Expansive Soils: Stouffer's Inn, Denver, Colorado, Vol 1*, June 16-18, ASCE New York, N.Y.

Spaans, E. J., & Baker, J. M. (1996). The soil freezing characteristic: Its measurement and similarity to the soil moisture characteristic. *Soil Science Society of America Journal*, 60(1), 13-19.

Sridharan, A., Sreepada Rao, A. & SivapuUaiah, P.V. (1986). Swelling pressure of clays. *Geotechnical Testing Journal, GTJODJ, 9*(1): 24-33.

Style, R. W., Peppin, S. S., Cocks, A. C., & Wettlaufer, J. S. (2011). Ice-lens formation and geometrical supercooling in soils and other colloidal materials. *Physical Review E*, 84(4), 041402.

Subba Rao, K. S. & Tripathy, S. (2003). Effect of aging on swelling & swell-shrink behavior of a compacted expansive soil. *ASTM Geotechnical Testing Journal, 26*(1): 36-46.

Sullivan, R. A. & McClelland, B. (1969). Predicting heave of buildings on unsaturated clay. *Proc. 2nd Int. Res. Eng. Conf. Expansive Soils*. Texas A & M Univ. Press, College Station, TX, pp. 404-420.

Sun, Xi, et al. (July 2017). "Evaluation and Comparison of Methods for Calculating Thornthwaite Moisture Index." *Australian Geomechanics Journal*.

Taber, S. (1930). The mechanics of frost heaving. *The Journal of Geology*, 38(4), 303-317.

Taylor, G. S., & Luthin, J. N. (1978). A model for coupled heat and moisture transfer during soil freezing. *Canadian Geotechnical Journal*, 15(4), 548-555.

Teng, T. C. P. & Clisby, M. B. (1975). Experimental work for active clays in Mississippi. *Transport. Eng. J. ASCE 101 (TEI)*: 77-95.

Teng, T. C. P., Mattox, R. M. & Clisby, M. B. (1972). *A study of active clays as related to highway design*. Research & Development Division, Mississippi State Highway Dept., Engineering & Industrial Research Station, Mississippi State University, MSHD-RD-72-045, pp: 134.

Teng, T. C. P., Mattox, R. M. & Clisby, M. B. (1973). Mississippi's experimental work on active clays. *Proc. Workshop on Expansive Clays & Shales in Highway design & Construction*. (pp 1-17). Univ. of Wyoming, Laramie.

Thomas, H. R., Cleall, P. J., Li, Y., Harris, C., & Kern-Luetschg, M. (2009). Modelling of cryogenic processes in permafrost and seasonally frozen soils. *Geotechnique*, 59(3), 173-184.

Thornthwaite, C. (1948). "An Approach Toward A Rational Classification of Climate", Geographical Review, Vol. 38, No. 1, pp. 55-94.

Thornthwaite, C. and Mather, J. (1955). "The Water Balance", Publications in Climatology, Vol. 8, No. 1.

Tu, H. (2015). Prediction of the variation of swelling pressure & 1-d heave of expansive soils with respect to suction. (M.S. Thesis). Department of Civil Engineering, Faculty of Engineering, University of Ottawa, Ottawa, Ontario, Canada, 191 p.

Tu, H. & Vanapalli, S.K. (2016). Prediction of the variation of swelling pressure & one-dimensional heave of expansive soils with respect to suction using the soil-water retention curve as a tool. *Canadian Geotechnical Journal, 53, NRC Research Press*, 1213-1234

TxDOT-124-E (1978). Method for Determining the Potential Vertical Rise, PVR. Texas Department of Transportation.

Ulldtz, P. (1987). Pavement analysis. Elsevier.

Van Der Merwe, D.H. (1964). The prediction of heave from the plasticity index & percentage clay fraction of soils. *Civil Engineers in South Africa,* 6: 337-42.

Vanapalli, S. and Lu, L. (2012). A State-of-the Art Review of 1-D Heave Prediction Methods for Expansive Soils. *International Journal of Geotechnical Engineering, 6*(1), 15-41.

Vanapalli, S. K. (1994). Simple Test Procedures and their Interpretation in Evaluating the Shear Strength of an Unsaturated Soil (Doctoral thesis, University of Saskatchewan, Canada, 1994).

Vann, Jeffry D. (2019) "A Soil Suction-Oedometer Method and Design Soil Suction Profile Recommendations for Estimation of Volume Change of Expansive Soils." *Arizona State University*, Tempe, AZ.

Vann, Jeffry D, and Houston, S. (2021) "Field Suction Profiles for Expansive Soil." doi:10.1061/(ASCE)GT.1943-5606.0002570.

Vann, J., Houston, S., Houston, W., Singhar, S., Cuzme, A. and Olaiz, A. (2018). A soil suction surrogate & its use in the suction-oedometer method for computation of volume change of expansive soils. *Proc. of the 7th International Conference on Unsaturated Soil.* (pp 1205-1210). Hong Kong.

Weston, D. J. (1980). Expansive roadbed, treatment for Southern Africa. *Proceeding of the 4th International Conference on Expansive Soils, 1*: 339-360.

Witczak, M.W., Zapata, C.E. and Houston, W.N. (2006). Models Incorporated into the Current Enhanced Integrated Climatic Model: NCHRP 9-23 Project Findings and Additional Changes after Version 0.7. Final Report. Project NCHRP 1-40D.

Wong, H. Y and Yong, R.M. (1973). A study of swelling & swelling force during unsaturated flow in expansive soils. *Proc. 3rd Int. Conf. Expansive Soils, Haifa, Israel, 1*: 143-151.

Wray, W.K. (1989). Mitigation of damage to structures supported on expansive soils. *Final Report, National Science Foundation. Vol. 1.*

Wray, W.K. and Meyer, K.T. (2004). Expansive Clay Soil- A Widespread & Costly GeoHazard. *GeoStrata, ASCE Geo-Institute, Vol. 5*, No.4. (pp 24-28).

Yoder, El. J., and M. W. Witczak, (1975). "Principles of Pavement Design" John Wiley & Sons.

Yue, Er, et al. (2014). "Climatic Parameter TMI in Subgrade Soils." *Climatic Parameter TMI in Subgrade Soils | Climatic Effects on Pavement and Geotechnical Infrastructure*.

Zareie, Alireza, et al. (2016). Thornthwaite Moisture Index Modeling to Estimate the Implication of Climate Change on Pavement Deterioration. *Journal of Transportation Engineering*, vol. 142, no. 4.

Zapata C. E. (1999) "Uncertainty in Soil-Water-Characteristic Curve and Impacts on Unsaturated Shear Strength Predictions." PhD Dissertation, *Arizona State University*, Arizona, USA.

Zapata, C.E. (2018). Empirical Approach for the Use of Unsaturated Soil Mechanics in Pavement Design. *Geotechnical Special Publication, Proceedings of the Second Pan-American Conference on Unsaturated Soils*. Nov. 11-14, 2017, Dallas, Texas. DOI: 10.1061/9780784481677.008, GSP 300, pp. 149-173.

Zapata, C.E., and Houston, W.N. (2009). Application of Unsaturated Soil Mechanics to Pavement Subgrade Design, *Geo-Strata*, Geo-Institute, American Society of Civil Engineers, May/June Issue. 3 pgs.

Zapata, C.E., Houston, W.N., Houston, S.L., and Walsh, K.D. (2000). Soil-Water Characteristic Curve Variability. In C.D. Shackelford, S.L. Houston, & N-Y Chang (eds), *Advances in Unsaturated Geotechnics. Geotechnical Special Publication No. 99*. Also *Proceedings of Sessions of Geo-Denver 2000*, August 5-8, 2000, Denver: ASCE Geo-Institute. pp. 84-124.

Zhang, Y. and Michalowski, R.L. (2015). Thermal-hydro-mechanical analysis of frost heave and thaw settlement. *Journal of Geotechnical and Geoenvironmental Engineering*, 141(7), 04015027.

Zhou, M.M. and Meschke, G. (2013). A three-phase thermo-hydro-mechanical finite element model for freezing soils. *International Journal for Numerical and Analytical Methods in Geomechanics*, 37(18), 3173-3193.